I.J.S.S. submitted Aug. 1996

MODELING OF THIN LAYER EXTENSIONAL THERMOELECTRIC SMA ACTUATORS

by

D. C. Lagoudas and A. Bhattacharyya

Center for Mechanics of Composites

Aerospace Engineering Department

Texas A & M University

College Station, TX 77843-3141

ABSTRACT

As a first step towards the design of a high frequency, high force, large strain shape memory alloy(SMA) actuator, we model in this work a thermoelectrically cooled thin SMA layer linear actuator. The SMA is subjected to cyclic phase transition between the martensitic and austenitic phases by alternate heating/cooling, achieved with the thermoelectric Peltier effect of a pair of P/N semiconductors. The effect of variable actuating load and constant load applied as boundary conditions on the SMA actuator are considered. The thermomechanical boundary value problem involves strongly coupled thermal and mechanical fields. The evolution equations for the field variables are integrated using the fourth-order Runge Kutta method and the coupling between the fields is accounted for by implementing an interative scheme. The primary parameters of interest in this work are the frequency response and evolution of the variable load. The performance of the actuator is compared with various commercially available actuators based on energy conversion efficiencies and energy output per unit volume of active material. Results of the analysis indicate that thin SMA layers($\approx 6\mu$ thick) under partial phase transformation are capable of delivering frequencies of about 30 Hz at peak stresses of about 145 MPa.

1. INTRODUCTION

An important issue related to the dynamic response of structures is the suppression of undesirable vibrations. This has motivated the study of high frequency, low force, low strain actuators using piezoelectrics, magnetostrictive or ferroelectric materials(Takagi,1990, Wada *et.al.*,1990, Giurgiutiu *et.al.*,1995). Of more recent origin is the study of certain large strain actuators which rely on the unique solid-solid phase transformation of shape memory alloys(SMA)(Wayman,1983). The phase transformation is highly sensitive to an applied thermomechanical loading and if the imposed stresses are reasonably high, significant deformations can be generated. For example, the corresponding actuation forces and deformations are at least 2 orders of magnitude higher than piezoelectrics. The shape memory effect is most significant in Nitinol which is composed of 50 at.wt.% each of Nickel(Ni) and Titanium(Ti)(or 55% and 45% by weight of Ni and Ti) respectively.

DISCLAIMER NOTICE

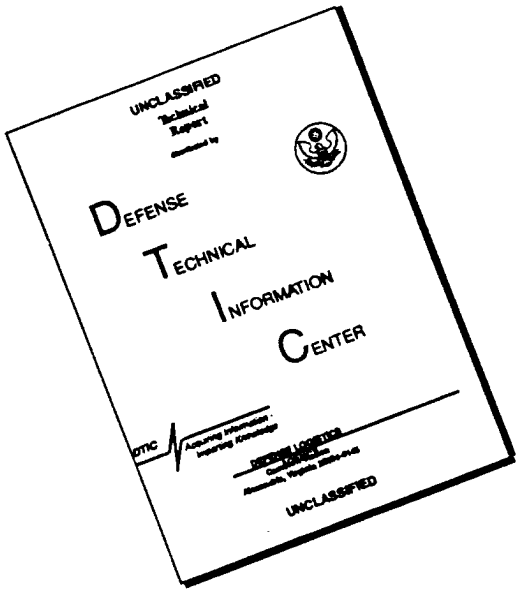

THIS DOCUMENT IS BEST QUALITY AVAILABLE. THE COPY FURNISHED TO DTIC CONTAINED A SIGNIFICANT NUMBER OF PAGES WHICH DO NOT REPRODUCE LEGIBLY.

The phase transformation in a Ni-Ti SMA is accompanied by a significant exchange of latent heat with the environment. The rate of the transformation is controlled solely by the time rate of heat transfer between the SMA and its environment. Conventional heat exchange mechanisms of resistive heating and forced convection cooling are slow and hence lead to a low frequency response for SMA actuators(Bo and Lagoudas,1994). A novel idea to increase the frequency of a SMA actuator was put forth by Lagoudas and Kinra(1993). They proposed to employ the heat transfer due to the thermoelectric Peltier effect(Domenciali,1954) which occurs between the junction of dissimilar metals due to the flow of electric current; depending on the current direction, one junction becomes cold and the other becomes hot. They suggested that the SMA be used directly as one of the junctions, which can then be heated or cooled by alternating the current direction.

To demonstrate this principle, consider a simple SMA actuator shown in Fig.1. A thin plate of SMA is used as a junction by sandwiching it between a pair of positively doped(P) and negatively doped(N) semiconductors. The other junction can be collectively represented by heat sinks(not shown) positioned at the ends of the P and N. If the SMA layer is mechanically constrained at the sides and the phase transformation is triggered on heating, an actuating stress, $\sigma(t)$, is produced.

Historically, thermoelectric coolers have been used primarily as refrigerators and thus it was their steady state cooling capability that was of interest. Recently, Thrasher *et.al.*(1992) have theoretically addressed some issues related to the study of the transient thermoelectric phenomenon; a comprehensive study however appeared to be lacking. This prompted Bhattacharyya *et.al.*(1995) to extensively study the transient thermoelectric problem in absence of actuation(no mechanical constraints on the SMA) for the configuration shown in Fig.1. They assumed that the temperature field is one-dimensional(along the z-axis), and found that due to the high thermal diffusivity of a Ni-Ti SMA, the temperature gradients in a thin SMA layer are negligible. With a view to investigating periodic solutions of thermal cycling(alternate heating and cooling), Lagoudas and Ding(1995) reexamined the same problem by assuming at the outset a 1-D temperature field in the P/N elements and a *uniform* temperature field in the SMA. In this paper, we extend their study to the issue of the thermoelectromechanical response where the actuator depicted in Fig.1 is subjected to a mechanical load boundary condition. The semiconductors are assumed to be stress-free whereas the stress state in the SMA is taken to be uniaxial(along the x-direction).

It is assumed that the SMA is thermoelastic. There are several constitutive models which have been proposed to characterize the thermomechanical response of a polycrystalline SMA during phase transformation. A non-exclusive list is the work of Tanaka(1986), Patoor, Eberhardt and Berveiller(1987), Liang and Rogers(1990,1991), Sun and Hwang(1993a,b). Recently, Boyd and Lagoudas(1995) proposed a phenomenological thermodynamic theory modeling an idealized SMA response. Lagoudas, Bo and Bhattacharyya(1996) extended it to model the gradual transformation of SMA polycrystals. We shall use the latter in this work. The resulting actuation stress $\sigma(t)$ of the actuator and its frequency response are the primary parameters of interest. The frequency range

studied is moderate enough so that inertial effects can be neglected. Another issue of interest is the coupling between the thermal and mechanical fields in the SMA during the phase transformation.

The outline of this paper is as follows. Sec.2 presents the general thermoelectromechanical governing equations. Sec.3 presents the thermomechanical boundary value problem for the SMA layer whereas Sec.4 gives the thermoelectric boundary value problem for the P/N semiconductors. Sec.5 summarises the thermoelectromechanical equations pertaining to the system depicted in Fig.1, Sec.6 presents the results of a parametric study and is followed by Sec.7 on the conclusions.

The scientific notation used in the text will be now described. Vectors will be denoted with a bold face, lower case Latin letter(except for the symbolic vector operator del, ∇) ; the symbol $\boldsymbol{n}$ will be reserved for a unit vector. The scalar product of two vectors, $\boldsymbol{x}$ and $\boldsymbol{n}$, is denoted by $\boldsymbol{x}.\boldsymbol{n}$ and it has the evaluation $x_i n_i$ in terms of components where indicial notation has been used and the Einstein summation convention is implied. On the other hand, their tensor product is denoted $\boldsymbol{x} \otimes \boldsymbol{n}$, or in indicial notation as $x_i n_j$, resulting in a second order tensor. Magnitude of a vector,$\boldsymbol{x}$, will be denoted as $|\boldsymbol{x}| = (\boldsymbol{x}.\boldsymbol{x})^{1/2}$. Second order tensors will be denoted with a bold face, lower case Greek letter and fourth order tensors will be denoted with upper case, bold face Latin letter. The trace of a second order tensor, $\boldsymbol{\sigma}$, is denoted $\mathrm{tr}(\boldsymbol{\sigma})$ and in indicial notation is given by σ_{ii}. The product of $\boldsymbol{\sigma}$ with a vector $\boldsymbol{v}$ is $\boldsymbol{\sigma v}$, or in indicial notation $\sigma_{ij} v_j$. The product of two second order tensors, $\boldsymbol{\sigma}$ and $\boldsymbol{\lambda}$, is denoted $\boldsymbol{\sigma\lambda}$ and its evaluation in indicial notation is $\sigma_{ik}\lambda_{kj}$. Their scalar product is defined as $\boldsymbol{\sigma}:\boldsymbol{\lambda} = \mathrm{tr}(\boldsymbol{\sigma\lambda}^T)$(superscript T indicates transpose). The tensor product of the two second order tensors is denoted $\boldsymbol{\sigma} \otimes \boldsymbol{\lambda}$, or in components as $\sigma_{ij}\lambda_{kl}$, resulting in a fourth order tensor. The inverse of any quantity, $\mathcal{A}$, will be denoted as $\mathcal{A}^{-1}$ and the material derivative will be denoted as $\dot{\mathcal{A}}$. While the indicial notation has been used in describing the mathematical notation, the various tensor operations in the text will be described solely by symbolic manipulation of the vector and tensor quantities.

2. THE THERMOELECTROMECHANICAL GOVERNING EQUATIONS

2.1 The Conservation Laws

Consider a given mass of the material occupying instantaneously a volume V surrounded by the surface S. We shall assume that body forces are negligible and ignore inertial effects(implying that the frequency of actuation is moderate; we shall address this issue in Sec.6.2 on "Parametric Studies"). For a particle occupying the position $\boldsymbol{x}$ in V at time t, the equations of motion, resulting from the conservation of linear momentum, reduce in the absence of applied body forces and inertial effects, to the equilibrium equations

$$\mathrm{div}\ \boldsymbol{\sigma} = 0\ , \tag{2.1}$$

where $\boldsymbol{\sigma} \equiv \boldsymbol{\sigma}(\boldsymbol{x}, t)$ is Cauchy's stress tensor. The angular momentum is also conserved, leading to the symmetry of the Cauchy stress tensor. We shall restrict the analysis to the study of SMA materials for which its mass density remains unchanged as it undergoes a phase transformation between its two crystalline phases of austenite and martensite. This assumption is reasonable as the phase transformation in SMAs is primarily a shear process(Delaey *et.al.*,1974). The conservation of mass is then trivially satisfied.

The conservation of energy is given by

$$\rho_{sma}\dot{u} = -\nabla.\boldsymbol{q} + r + \boldsymbol{\sigma} : \dot{\boldsymbol{\epsilon}} \ , \tag{2.2}$$

where ρ_{sma} is the mass density of the SMA material, $\dot{u} \equiv \dot{u}(\boldsymbol{x}, t)$ is the specific internal energy rate(i.e. internal energy rate per unit mass), $\boldsymbol{q} \equiv \boldsymbol{q}(\boldsymbol{x}, t)$ is the energy flux vector(use of the words "energy flux" instead of the familiar "heat flux" is relevant in the context of thermoelectricity, to be explained later) and $r \equiv r(\boldsymbol{x}, t)$ is the heat source per unit volume. The strain rate tensor is denoted $\dot{\boldsymbol{\epsilon}} \equiv \dot{\boldsymbol{\epsilon}}(\boldsymbol{x}, t)$, given for small strain rates and rotations by

$$\dot{\boldsymbol{\epsilon}} = \frac{1}{2}\left[(\nabla \otimes \dot{\boldsymbol{u}}) + (\nabla \otimes \dot{\boldsymbol{u}})^T\right] \ , \tag{2.3}$$

in terms of the rate of the displacement vector $\dot{\boldsymbol{u}} \equiv \dot{\boldsymbol{u}}(\boldsymbol{x}, t)$(not to be confused with the scalar, u, used to denote the specific internal energy). This is a reasonable assumption even for deformations during phase transformation in a polycrystalline SMA where the total strains usually do not exceed 8%(Delaey *et.al.*,1974).

As we shall see later, the energy flux depends on the current density vector, $\boldsymbol{j} \equiv \boldsymbol{j}(\boldsymbol{x}, t)$. This implies the consideration of conservation of charge, stated as

$$\frac{\partial \rho_c}{\partial t} + \nabla.\boldsymbol{j} = 0 \ , \tag{2.4}$$

where $\rho_c \equiv \rho_c(\boldsymbol{x}, t)$ is the net charge per unit volume. While electrical transients will occur as a current density is applied at $t = 0$, it is expected that the time interval over which these transients vanish will be infinitesimal compared to that of the transients in the thermal and mechanical fields. Based on this observation, also made by Lagoudas and Ding(1995), we shall assume that $\frac{\partial \rho_c}{\partial t} = 0$. We then have

$$\nabla.\boldsymbol{j} = 0 \ . \tag{2.5}$$

2.2. Thermoelectromechanical Constitutive Equations

2.2.1 *The Shape Memory Alloy*

The thermomechanical constitutive response of the SMA is given in the rate form by

$$\dot{\boldsymbol{\epsilon}} = \dot{\boldsymbol{\epsilon}}^{el} + \dot{\boldsymbol{\epsilon}}^{th} + \dot{\boldsymbol{\epsilon}}^{t} = \dot{\boldsymbol{M}}\boldsymbol{\sigma} + \boldsymbol{M}\dot{\boldsymbol{\sigma}} + \dot{\boldsymbol{\epsilon}}^{th} + \dot{\boldsymbol{\epsilon}}^{t} \ , \tag{2.6}$$

where $\dot{\epsilon}$, $\dot{\epsilon}^{el}$, $\dot{\epsilon}^{th}$ and $\dot{\epsilon}^{t}$ are the rates of the total strain, elastic strain, thermal strain and inelastic strain due to phase transformation, respectively. The fourth order effective elastic compliance tensor of the polycrystalline SMA material is denoted as M and will be defined in Eq.(2.9) below.

The thermal and inelastic strain rates are(Boyd and Lagoudas,1995)

$$\dot{\epsilon}^{th} = \alpha^{th}\dot{T} + \dot{\alpha}^{th}\Delta T \quad \text{and} \quad \dot{\epsilon}^{t} = \lambda\dot{\xi} \ , \tag{2.7}$$

where α^{th} is the coefficient of thermal expansion second order tensor, T is the temperature, $\Delta T = T - T_0$ with T_0 being a reference temperature and the second order tensor λ defines the "direction" in which the inelastic strains develop during the phase transformation. The constituent phases of austenite(A) and martensite(M) for polycrystalline SMA are assumed to have isotropic compliances and coefficient of thermal expansion tensors. Therefore

$$M_i = \frac{1}{E_i}I + \frac{\nu_i}{E_i}(I - \delta \otimes \delta) \ , \quad \alpha_i^{th} = \alpha_i^{th}\delta \ , \tag{2.8}$$

where E_i, ν_i and α_i^{th} are the Young's modulus, Poisson's ratio and the coefficient of thermal expansion, respectively for the ith phase. I and δ are the fourth order and second order identity tensors respectively.

For simplicity, the corresponding effective properties of the SMA are approximated by the rule of mixtures as(Boyd and Lagoudas,1995)

$$M \equiv M(\xi) = M_A + \xi\Delta M \quad \text{and} \quad \alpha \equiv \alpha^{th}(\xi) = \alpha_A^{th} + \xi\Delta\alpha^{th} \ , \tag{2.9}$$

where $\Delta M = M_M - M_A$ and $\Delta\alpha^{th} = \alpha_M^{th} - \alpha_A^{th}$. A comparison with the Mori-Tanaka averaging scheme, as discussed by Boyd and Lagoudas(1995) for a polycrstalline SMA has shown that the above approximation is adequate. The tensor λ is assumed to have the following representation(Boyd and Lagoudas,1995)

$$\lambda = \frac{3}{2}H\frac{1}{\sigma_e}\sigma' \ , \ \dot{\xi} > 0 \quad \text{and} \quad \lambda = H\frac{1}{\epsilon_e^{t,p}}\epsilon^{t,p} \ , \ \dot{\xi} < 0 \ , \tag{2.10}$$

where H is the maximum uniaxial transformation strain, $\sigma_e = \left(\frac{3}{2}\sigma' : \sigma'\right)^{1/2}$, $\sigma' = \sigma - \frac{1}{3}tr(\sigma)\delta$ and $\epsilon^{t,p}$ is the inelastic phase transformation strain before the $M \rightarrow A$ phase transformation commences, with $\epsilon_e^{t,p} = \left(\frac{2}{3}\epsilon^{t,p} : \epsilon^{t,p}\right)^{1/2}$. The evolution of the volume fraction of martensite $\dot{\xi}$ is given by(Boyd and Lagoudas,1995)

$$\dot{\xi} = \left[\sqrt{\rho_{sma}\frac{\partial\Delta u(\xi)}{\partial\xi}}\right]^{-1}\left(\psi\dot{T} + \beta : \dot{\sigma}\right) \ , \tag{2.11}$$

where $\psi \equiv \psi(\xi), \beta \equiv \beta(\xi, \sigma, T)$. The explicit forms of ψ and β are

$$\psi(\xi) = \frac{\rho_{sma}\Delta s}{\sqrt{\rho_{sma}\frac{\partial\Delta u(\xi)}{\partial\xi}}} \quad , \quad \beta(\xi, \sigma, T) = \frac{\Delta M\sigma + \Delta\alpha^{th}\Delta T + \lambda}{\sqrt{\rho_{sma}\frac{\partial\Delta u(\xi)}{\partial\xi}}} \ . \tag{2.12}$$

In the above expressions $\Delta s = s_M - s_A$ and $\Delta u(\xi) = u_M(\xi) - u_A(\xi)$; s_i is the average specific entropy and $u_i(\xi)$ is the internal energy of the ith phase at the reference state that corresponds to $\sigma = 0$ and $T = T_0$.

Eqs.(2.7),(2.8) and (2.11) in Eq.(2.6) result in

$$\dot{\epsilon} = M_T \dot{\sigma} + \alpha_T^{th} \dot{T} \ , \tag{2.13}$$

where M_T is the tangent compliance fourth-order tensor and α_T^{th} is the tangent coefficient of thermal expansion second-order tensor during the transformation.These are given by

$$\begin{aligned} M_T &\equiv M_T(\xi, \sigma, T) = M(\xi) + \beta(\xi, \sigma, T) \otimes \beta(\xi, \sigma, T) \ , \\ \alpha_T^{th} &\equiv \alpha_T^{th}(\xi, \sigma, T) = \alpha^{th}(\xi) + \psi(\xi)\beta(\xi, \sigma, T) \ , \qquad \dot{\xi} \neq 0 \ . \end{aligned} \tag{2.14}$$

In absence of transformation(i.e. $\dot{\xi} = 0$), we set $\beta(\xi, \sigma, T) = 0$ and $\psi(\xi) = 0$ in the above expressions.

During phase transformation, Eq.(2.2) becomes(Boyd and Lagoudas,1995)

$$-\nabla . q + r = C\dot{T} + T\alpha^{th} : \dot{\sigma} + \gamma\dot{\xi} \ , \tag{2.15}$$

where for simplicity, the effective heat capacity, C, is given by the rule of mixtures(Boyd and Lagoudas,1995) as $C \equiv C(\xi) = C_A + \xi(C_M - C_A)$, and C_i is the effective heat capacity of the ith phase. Note that in absence of phase transformation,i.e. $\dot{\xi} = 0$, the conservation of energy equation (2.15) reduces to the well known form for a thermoelastic material(Boley and Weiner,1960). It is known that the thermoelastic coupling term, $T\alpha^{th} : \dot{\sigma}$, is negligibly small during quasistatic mechanical loading(Boley and Weiner,1960). With phase transformation however, additional thermomechanical coupling terms are introduced through the term $\gamma\dot{\xi}$(as $\dot{\xi}$ is dependent on $\dot{T}$ and $\dot{\sigma}$; see Eq.(2.11)). We shall investigate this coupling in Sec.5.4. The parameter, γ, in Eq.(2.15), is given by

$$\gamma(\sigma, T) = T\sigma : \Delta\alpha^{th} + \rho_{sma}\Delta s T - \Pi \ , \tag{2.16}$$

where Π is the thermodynamic driving force for the phase transformation and is given by

$$\Pi = \frac{1}{2}\sigma : \Delta M \sigma + \sigma : (\Delta\alpha^{th}\Delta T + \lambda) + \rho_{sma}\Delta s T - \rho_{sma}\Delta u(\xi) \ . \tag{2.17}$$

During the phase transformation, Π attains the material threshold value Y

$$\Pi \overset{+}{=} Y \quad \text{for} \quad \dot{\xi} \gtrless 0 \ , \ \ Y > 0 \ . \tag{2.18}$$

The method of determination of the parameters $\rho_{sma}\Delta s$, $\rho_{sma}\Delta u(\xi)$ in Eq.(2.12) and Y in Eq.(2.18) from experiments are given in Sec.A of the Appendix.

2.2.2 *Thermoelectric Materials*

There is no phase transformation involved in a thermoelectric material. Thus Eq.(2.2) simply becomes the heat conduction equation(Boley and Weiner,1960)

$$-\nabla.q + r = C\dot{T} \ , \tag{2.19}$$

for a stress-free material(we shall return to this point in Sec.4.1).

In order to give the constitutive equations of thermoelectricity, we start with the definition of the energy flux vector(Domenciali,1954)

$$q = q^{th} + q^{el} \quad , \quad q^{th} = -\kappa\nabla T \quad , \quad q^{el} = (\alpha T + \frac{1}{q_c}\bar{\mu}I)j \ , \tag{2.20}$$

where the vectors q^{th} and q^{el} are the thermal and electrical components of the energy flux vector respectively. The former is taken to relate to the temperature gradient through the Fourier law of heat conduction. κ is the second order tensor of thermal conductivity and α is the second order tensor of Seebeck coefficients(representing the phenomenon of thermoelectricity). We point out that the temperature T used in the statement of q^{el} is in degrees Kelvin, as required by the theory of thermoelectricity(Domenciali, 1954); q_c is the particle charge and $\bar{\mu}$ is the electrochemical potential. The electrical current density, j, is (Domenciali,1954)

$$j = -\rho^{-1}(\frac{1}{q_c}\nabla\bar{\mu} + \alpha^T\nabla T) \ , \tag{2.21}$$

where ρ is the second order tensor of electrical resistivity, $\nabla\bar{\mu} = \nabla\mu - q_c e$ where μ is the chemical potential and e is the electric field vector. Note that using Eq.(2.20), the term $\nabla.q$ in Eq.(2.19) becomes

$$-\nabla.q = \kappa : (\nabla\otimes\nabla T) + \text{div}\ \kappa.\nabla T - \alpha^T\nabla T.j - (\alpha : \nabla\otimes j)T - (\text{div}\ \alpha^T.j)T \\ -\frac{1}{q_c}(\nabla\bar{\mu}.j - \bar{\mu}\nabla.j) \ . \tag{2.22}$$

Of particular interest to this analysis is an isotropic, homogeneous material for which the heat conduction equation is simplified considerably. For an isotropic material,

$$\rho = \rho i \quad , \quad \kappa = \kappa i \quad , \quad \alpha = \alpha i \ . \tag{2.23}$$

If these properties are assumed to be spatially uniform and insensitive to temperature variations, then

$$\nabla\rho = 0 \quad , \quad \nabla\kappa = 0 \quad , \quad \nabla\alpha = 0 \ . \tag{2.24}$$

With Eqs.(2.23)-(2.24), div $\kappa = \nabla\kappa = 0$, div $\alpha^T = \nabla\alpha = 0$. These simplifications, along with Eqs.(2.5) and (2.21), result in

$$-\nabla.q = -\nabla.q^{th} + \rho|j|^2 = \kappa\nabla.\nabla T + \rho|j|^2 \ . \tag{2.25}$$

It is seen that the Joule heating term, $\rho|j|^2$, has emerged as a part of $-\nabla.q$. The parameter r in Eq.(2.15) is then interpreted as collectively representing all heat sources except Joule heating. In the next section, the thermomechanical boundary value problem(BVP) for the SMA layer is presented.

3. THE THERMOMECHANICAL BOUNDARY VALUE PROBLEM FOR THE THIN SMA LAYER

For convenience, we present the mechanical BVP and the thermal BVP separately in Secs.3.1 and 3.2 respectively. In either case, as the corresponding conservation laws(i.e.governing equations) have been already introduced in Sec.2.1, the relevant boundary conditions and assumptions to simplify the problem will now be presented.

3.1 The Mechanical Boundary Value Problem

Based on the specific geometry of the thin SMA layer depicted in Fig.1, we assume the following boundary conditions based on a cartesian coordinate system with its origin at the center of the SMA layer.

$$\boldsymbol{u}.\boldsymbol{n} = u_s(t) \quad , \quad \int \boldsymbol{\sigma}\boldsymbol{n}\, dA = k_s\left(\delta_0 - u_s(t)\right)\boldsymbol{n} \quad \text{at} \quad x = \stackrel{+}{-}\frac{w}{2} \quad , \tag{3.1}$$

$$\boldsymbol{\sigma}\boldsymbol{n} = 0 \quad \text{at} \quad y = \stackrel{+}{-}\frac{b}{2}\ ,\ z = \stackrel{+}{-}\frac{d}{2}\ , \tag{3.2}$$

where the vector $\boldsymbol{n}$ is taken as the outward unit normal to the surface of the SMA; b,d and w are the dimensions of the SMA, as indicated in Fig.1. The first two conditions of the above represent a spring loaded boundary condition at $x = \stackrel{+}{-}\frac{w}{2}$; $u_s(t)$ is assumed to be spatially uniform, the spring has a stiffness k_s and an initial stretch δ_0. The remaining surfaces are taken to be traction-free and thus includes the assumption of a frictionless interface between the P/N. The temperature and the martensitic volume fraction are taken as initially uniform in the SMA layer

$$T = T_0 \quad \text{and} \quad \xi = \xi_0 \quad \text{at} \quad t = 0\ . \tag{3.3}$$

We shall also assume that the initial thermal and inelastic strains are

$$\epsilon^{th} = 0 \ \text{ and } \ \epsilon^t = 0 \quad \text{at} \quad t = 0\ . \tag{3.4}$$

Denoting σ_{xx} as the normal component of $\boldsymbol{\sigma}$ in the x-direction, it is seen that the following uniaxial stress field

$$\sigma_{xx} \equiv \sigma_{xx}(y, z, t)\ , \tag{3.5}$$

with all other components of $\boldsymbol{\sigma}$ being zero, satisfies the equilibrium equation (2.1) and the traction-free boundary conditions of Eq.(3.2).

At this point, we make a simplifying assumption that the temperature field is spatially uniform in the SMA layer

$$T \equiv T(t) \ . \tag{3.6}$$

The rationale behind the above assumption will be discussed in Sec.3.2 on "The Thermal Boundary Value Problem". With the latter of Eq.(3.3), and Eqs.(3.5)-(3.6), it can be easily inferred from Eq.(2.11) that $\xi \equiv \xi(y,z,t)$. This in turn implies from Eq.(2.14) that M_T and $\boldsymbol{\alpha}_T$, like σ_{xx}, are independent of x and as a consequence, we conclude from Eq.(2.13) that $\dot{\boldsymbol{\epsilon}} \equiv \dot{\boldsymbol{\epsilon}}(y,z,t)$. Therefore, in absence of rigid body motion,

$$\dot{u}_x = \dot{\epsilon}_{xx}\ x \ , \tag{3.7}$$

following from Eq.(2.3); $\dot{u}_x$ is the rate of displacement of a particle in the x-direction and $\dot{\epsilon}_{xx}$ is the normal component of the strain rate, $\dot{\boldsymbol{\epsilon}}$, in the x-direction. With the first of Eq.(3.1)(recall the assumption that $u_s(t)$ is spatially uniform), we note that $\dot{u}_s(t)(= \dot{\epsilon}_{xx}\frac{w}{2}$ from Eq.(3.7)) will be spatially uniform only if $\dot{\epsilon}_{xx}$ is; thus by Eq.(2.13), $\boldsymbol{\sigma}$(or its sole nonvanishing component σ_{xx}) will necessarily have to be spatially uniform. The resulting uniaxial stress field is denoted as

$$\sigma_{xx} \equiv \sigma(t) \ . \tag{3.8}$$

The above solution, applied to the second of Eq.(3.1), results in

$$\sigma(t) = \frac{k_s}{bd}(\delta_0 - u_s(t)) \ . \tag{3.9}$$

We now note that since both state variables, $T(t)$ and $\sigma(t)$, are spatially uniform, so is $\xi(t)$(inferred from Eq.(2.11) and the second of Eq.(3.3)). The preceding conclusions also imply the spatial uniformity of $\dot{\boldsymbol{\epsilon}}$ by Eq.(2.13) using which, with (3.7) and the rate form of Eq.(3.9), we have

$$\dot{\sigma}(t) = s(\xi,\sigma,T)\dot{T}(t) \ , \tag{3.10}$$

where

$$s(\xi,\sigma,T) = -\left[\frac{2bd}{w}\frac{E_T(\xi,\sigma,T)}{k_s} + 1\right]^{-1} E_T(\xi,\sigma,T)\alpha_T^{th}(\xi,\sigma,T) \ , \tag{3.11}$$

and

$$E_T(\xi,\sigma,T) = [E(\xi)^{-1} + \beta^2(\xi,\sigma,T)]^{-1} \quad \text{and} \quad \alpha_T^{th}(\xi,\sigma,T) = \alpha^{th}(\xi) + \psi(\xi)\beta(\xi,\sigma,T) \ .$$

$E(\xi)$ is the effective Young's modulus of the SMA layer, and $\beta(\xi,\sigma,T)$ is the normal component of the tensor $\boldsymbol{\beta}(\xi,\boldsymbol{\sigma},T)$ in the x-direction.

Thus among the three state variables, ξ, σ and T, the evolution of the first two are given by Eqs.(2.11) and (3.10) respectively. Evolution of the temperature field will follow from the conservation of energy for the SMA layer, to be given next in Sec.3.2.

Before we go on to the next section, we note that the initial values of the state variables are needed alongwith their evolution equations to compute their total values at a time t. While these have been prescribed for T and ξ by Eq.(3.3), the initial value of stress, $\sigma(0)$, will follow from the boundary conditions of Eqs.(3.1),(3.2) and the solution given by (3.8) respectively. At $t = 0$, using Eq.(2.6) for purely elastic behavior and with Eq.(3.4), we obtain

$$\epsilon(0) = \frac{1}{E(\xi_0)}\sigma(0) \ , \tag{3.12}$$

where the spatially uniform normal component, ϵ_{xx}, of $\dot{\epsilon}$ in the x-direction is denoted as $\epsilon(t)$. Combining the above with the total form of Eq.(3.7) and the second of Eq.(3.1), we have

$$\sigma(0) = \frac{k_s \delta_0}{bd + \frac{k_s w}{2E(0)}} \ . \tag{3.13}$$

3.2 The Thermal Boundary Value Problem

We now recall Eq.(3.6), wherein we made the assumption of an uniform temperature field in the SMA thin layer(thickness of the order of mm). This assumption has its origin in the transient thermoelectric problem addressed by Bhattacharyya *et.al.*(1995) in absence of actuation forces where a 1-D variation(along the z-axis) of temperature in the P/SMA/N geometry of Fig.1 was assumed. The assumption of a 1-D temperature field was verified by the finite element method and was found to be an excellent one. The method of separation of variables was invoked to solve the 1-D problem analytically. It was found that, as a consequence of the high thermal diffusivity of a Ni-Ti SMA, the temperature field was virtually uniform in the SMA layer. Lagoudas and Ding(1995), in an effort to find periodic solutions of a cyclic thermal field, addressed the same problem but assumed an uniform temperature field in the SMA at the outset. The analytical solution resulted in an integro-differential equation for the SMA temperature which they solved by a finite difference scheme. Prompted by these considerations, we also assume an uniform temperature field in the SMA; our formulation then is an extension of Lagoudas and Ding's(1995) work to the thermoelectromechanical case.

We assume that the electric current density vector is directed along the z-direction, such that

$$j = J(t)n_z \ . \tag{3.14}$$

The portion of the surface of the SMA in interfacial contact with the P/N elements is defined as S_I; the remainder of the surface is denoted as S_E. The thermal boundary condition on S_I is

defined as

$$\boldsymbol{q}^{th}.\boldsymbol{n} = q \quad \text{on} \quad S_I : \; z = \stackrel{+}{-} \frac{d}{2} \,, \tag{3.15}$$

where the heat flux q will come from the interface condition between the SMA and P/N and will be made explicit in Sec.4. A convective boundary condition is specified for the remaining surfaces of the SMA. Therefore

$$\boldsymbol{q}.\boldsymbol{n} = -h(T(t) - T_0) \quad \text{on} \quad S_E : \; x = \stackrel{+}{-} \frac{w}{2} \,, y = \stackrel{+}{-} \frac{b}{2} \,, \tag{3.16}$$

where h is the convection coefficient and T_0 is the ambient temperature. Note that the initial condition for the temperature is given by the first of Eq.(3.3).

We now write Eq.(2.15) alongwith Eq.(2.25) in an integral form and use Eqs.(3.6), (3.10), (3.16) and (3.14), to get

$$-\frac{1}{V_{sma}} \int_{S_I} q \; dS - 2h \left(\frac{1}{b} + \frac{1}{w} \right) (T(t) - T_0) + \rho J(t)^2 = \left\{ C(\xi) + \gamma(\sigma, T) \left[\sqrt{\rho_{sma} \frac{\partial \Delta u(\xi)}{\partial \xi}} \right]^{-1} \psi(\xi) + \right.$$
$$\left. \left[\alpha^{th}(\xi) T(t) + \gamma(\sigma, T) \left[\sqrt{\rho_{sma} \frac{\partial \Delta u(\xi)}{\partial \xi}} \right]^{-1} \beta(\xi, \sigma, T) \right] s(\xi, \sigma, T) \right\} \dot{T}(t) \,, \tag{3.17}$$

where the volume of the SMA layer is denoted as V_{sma} and the joule heating is accounted for by setting $r = \rho J(t)^2$ in Eq.(2.15), where ρ is the resistivity of the SMA. We now have three evolution equations for the state variables, ξ, σ and T given by Eqs.(2.11), (3.10) and (3.17) and these can be solved once the heat flux q in Eq.(3.17) is specified. This is done in Sec.4 next. We point out here that all quantities pertaining to the SMA have been denoted without any subscripts(except its density ρ_{sma}, volume, V_{sma} and mass, M_{sma}). In the next section where the thermoelectric problem for the P/N semiconductors will be discussed, all quantities pertaining to the P/N semiconductors will be labeled with the subscript P or N respectively.

4. THE THERMOELECTRIC BOUNDARY VALUE PROBLEM FOR THE SEMICONDUCTORS

As in the previous section for the SMA layer, we first present the boundary conditions for the semiconductors and certain relevant assumptions. Any simplification in the conservation laws, already presented in Sec.2.2, will then be discussed. We shall assume that the tractions are continuous at the interfaces of the SMA with P/N. Thus, by Eq.(3.2), we conclude that the interface is traction-free. Assuming that the remaining surfaces of the P/N elements are also traction-free, the mechanical boundary conditions for P/N become

$$\boldsymbol{\sigma} \boldsymbol{n} = 0 \;\; \text{on} \;\; S_i \quad (i = P, N) \,, \tag{4.1}$$

where S_i is the surface bounding the ith phase. The solution for the stress field in the P/N elements then follows simply as

$$\boldsymbol{\sigma} = 0 \ . \tag{4.2}$$

The temperature gradient and the current density vector are taken to be unidirectional(along the z-axis)(Bhattacharyya *et.al.*(1995); see discussion at the beginning of Sec.3.2). These conditions are summarized as

$$T = T_i(z,t) \quad \text{and} \quad \boldsymbol{j} = J(t)\boldsymbol{n}_z \qquad (i = P,N) \ . \tag{4.3}$$

An isothermal boundary condition is assumed at the end surfaces

$$T_i\left(\stackrel{+}{-}\frac{d}{2}\stackrel{+}{-}d_i,t\right) = T_0 \qquad (i = P,N) \ . \tag{4.4}$$

The interfaces between the SMA with P and N are taken to be thermally perfect, so that the temperature and the energy flux are continuous. These are stated respectively as

$$T(t) = T_i\left(\stackrel{+}{-}\frac{d}{2},t\right) \quad \text{and} \quad \boldsymbol{q}.\boldsymbol{n} = \boldsymbol{q}_i.\boldsymbol{n} \ \text{ at } \ z = \stackrel{+}{-}\frac{d}{2} \qquad (i = P,N) \ , \tag{4.5}$$

where $\boldsymbol{n}$ is an outward unit normal on the surface of P/N elements. We shall use the latter boundary condition shortly to give a discussion of the Peltier effect. A convective boundary condition is assumed for the remaining surfaces

$$\boldsymbol{q}_i.\boldsymbol{n} = -h(T_i(z,t) - T_0) \quad \text{on} \quad x = \stackrel{+}{-}\frac{w}{2} \ , y = \stackrel{+}{-}\frac{b}{2} \qquad (i = P,N) \ . \tag{4.6}$$

The initial condition for the temperature is taken as

$$T_i(z,0) = T_0 \quad (i = P,N) \ . \tag{4.7}$$

The conservation of energy equation will follow from Eq.(2.19) and Eq.(2.25) as

$$\kappa_i \nabla.\nabla T_i + \rho_i J^2(t) + r = C_i \dot{T}_i \qquad (i = P,N) \ . \tag{4.8}$$

The convection boundary condition given by Eq.(4.6) for the ith element is included approximately as a source term(refer Bhattacharyya *et.al.*,1995); thus $r = -2h\left(\frac{1}{b}+\frac{1}{w}\right)(T_i(z,t)-T_0)$. In addition, using Eq.(4.3), Eq.(4.8) then becomes

$$\kappa_i \frac{\partial^2 T_i}{\partial z^2}(z,t) + \rho_i J(t)^2 - 2h\left(\frac{1}{b}+\frac{1}{w}\right)(T_i(z,t)-T_0) = C_i \frac{\partial T_i}{\partial t}(z,t) \ , \quad (i = P,N) \ , \quad t > 0 \ , \tag{4.9}$$

where k_i, ρ_i and C_i are the thermal conductivity, the electrical resistivity and the heat capacity of the ith element respectively.

We now give a discussion of the Peltier effect based on the interface condition for the energy flux, given by the latter of Eq.(4.5). Starting with the SMA/P interface and assuming, i.e. $\bar{\mu} = \bar{\mu}_p$(Bhattacharyya *et.al.*,1995), the second of Eq.(4.5) with Eq.(2.20) is written for the SMA/P interface as

$$\left(\boldsymbol{q}^{th} - \boldsymbol{q}_p^{th}\right).\boldsymbol{n} = \left(\boldsymbol{q}_p^{el} - \boldsymbol{q}^{el}\right).\boldsymbol{n} \quad \rightarrow \quad \left(q^{th} - q_p^{th}\right).n_z = (\alpha_p - \alpha)T(t)\boldsymbol{j}.\boldsymbol{n}_z \ , \tag{4.10}$$

where $\boldsymbol{n} = -\boldsymbol{n}_z$. The Seebeck coefficients of the P and SMA are α_p and α respectively. The jump in the heat flux, denoted by Eq.(4.10), represents the thermoelectric Peltier effect. Note that this effect is driven by the electric current and influences the temperature gradients. This is exactly opposite to the thermoelectric Seebeck effect, based on which thermocouples operate. In this latter case, if the junctions between two dissimilar metals forming a closed circuit are maintained at two different temperatures, an electric current will flow. Both effects are controlled by the same parameter, i.e. the Seebeck coefficient(Harman and Honig,1967).

Returning to Eq.(4.10), the jump in the *heat flux* indicates that the Peltier effect has manifested itself as a heat source/sink at the interface. For commercially available Bismuth Telluride(Bi-Te) semiconductors, $\alpha_p = 2.15 \times 10^{-4} VK^{-1}$(Melcor,1992) whereas $\alpha = 1.2 \times 10^{-5} VK^{-1}$(Jackson *et.al.*,1972) for a Ni-Ti SMA and $\alpha_p - \alpha > 0$. We note that $T(t)$ has to be in absolute units(Domenciali,1954), i.e.$T(t) \geq 0$ for $t \geq 0$. Examining the right-hand side of Eq.(4.10), it is clear that when the current density vector is directed from the N to the P($\boldsymbol{j}.\boldsymbol{n}_z > 0$), we have $(\boldsymbol{q}^{th} - \boldsymbol{q}_p^{th}).\boldsymbol{n}_z > 0$. This implies that the heat lost by the SMA at the SMA/P interface is in excess of that which is conducted into the P. The difference, for the chosen current direction, represents the Peltier effect acting as a heat sink at the SMA/P interface. Should the current density be reversed, it is easy to deduce that the Peltier effect now acts as a heat source.

Let us now consider the situation at the SMA/N interface. With Eq.(2.20), the latter of Eq.(4.5) is written for this interface as

$$\left(\boldsymbol{q}^{th} - \boldsymbol{q}_n^{th}\right).\boldsymbol{n} = \left(\boldsymbol{q}_n^{el} - \boldsymbol{q}^{el}\right).\boldsymbol{n} \quad \rightarrow \quad \left(q^{th} - q_n^{th}\right).n_z = (\alpha_n - \alpha)T(t)\boldsymbol{j}.\boldsymbol{n}_z \ , \tag{4.11}$$

where $\boldsymbol{n} = \boldsymbol{n}_z$ and assuming $\bar{\mu} = \bar{\mu}_n$. For Bi-Te semiconductors $\alpha_n = -\alpha_p$(Melcor,1992); thus $\alpha_n - \alpha < 0$. From the above equation, we see that if the current is directed from the N to the P($\boldsymbol{j}.\boldsymbol{n}_z > 0$), then $\left(q^{th} - q_n^{th}\right).n_z < 0$. Thus, at the SMA/N interface, heat lost by the SMA is in excess of that which is conducted into the N. Therefore, the Peltier effect at this interface has a similar effect as at the SMA/P interface for the same current direction,i.e. it acts as a heat sink. When the current is reversed(P to N), the effect is opposite, but again similar at both interfaces, i.e. the Peltier effect acts as a heat source at both interfaces.

We note that when the current is directed from the N to the P, the heat lost to the Peltier heat sink at both interfaces has the potential to *cool* the SMA inspite of the fact that electrical current is being passed through the SMA(providing a Joule heat source). It was shown by Bhattacharyya

et.al.(1995) in their theoretical predictions and comparisons with experiments, that for a moderate current density and with a given geometry of P/SMA/N, the SMA can be indeed cooled by passing the current from the N to the P. The theoretical predictions however show that there is a critical current density above which it is not possible to cool the material(Lagoudas and Ding,1995) due to a substantial increase of Joule heating. If, however, the current was directed from P to N, the Peltier heat source reinforces the Joule heating; thus, for this current direction, heating occurs at all current densities. While semiconductors of various metals/alloys are available, commercially available Bi-Te has one of the highest magnitudes of α_p and α_n around room temperature and are thus capable of delivering the maximum thermoelectric effect(maximum heating/cooling)(Harman and Honig,1967,Pollock,1991)

Bhattacharyya *et.al.*(1995) and Lagoudas and Ding(1995) invoked symmetry considerations based on certain assumptions to simplify the mathematical problem. We shall do the same. The assumptions are listed below.

1. All material properties of the P and N Bi-Te semiconductors are assumed identical(Melcor,1992) except for their Seebeck coefficients which have equal magnitudes but opposite signs. Thus

$$\kappa_p = \kappa_n \ , \ \rho_p = \rho_n \ , \ C_p = C_n \ , \ \alpha_p = -\alpha_n \ . \tag{4.12}$$

2. Since for Bi-Te semiconductors and Ni-Ti SMAs, $\alpha_p = -\alpha_n \approx 18\alpha$, we assume

$$\alpha_p = -\alpha_n >> \alpha \qquad \rightarrow \qquad \alpha_p - \alpha \approx \alpha_p \ , \ \alpha_n - \alpha \approx \alpha_n .$$

The above assumption has been tested in a finite element computation of the thermoelectric problem. With the values of the Seebeck coefficients for P/SMA/N, the evolution of the temperature in the SMA was computed and compared with the case when α for the SMA was set to zero. The difference in the computed temperature over a time evolution of 30 sec was less than 0.5%. For the Seebeck coefficients of Bi-Te and Ni-Ti, the assumption is thus a sound one.

With the above assumptions, the 1-D temperature distribution is symmetrical about the plane, $z = 0$. This was shown analytically by Lagoudas and Ding(1995). Thus

$$T_p(z,t) = T_n(-z,t) \ , \ \frac{d}{2} \leq z \leq \frac{d}{2} + d_p \ , \ t > 0 \ . \tag{4.13}$$

With Eq.(4.13), only half of the P/SMA/N assemblage needs to be considered; we therefore shall focus on the P element only, i.e. in the remainder of the text, Eq.(4.9) will be considered only for the P element. We shall now combine the equations developed in Secs.3 and 4 and present them in their final form in the next section.

5. SOLUTION OF THE COUPLED THERMOELECTROMECHANICAL PROBLEM AND THE ENERGY CONVERSION EFFICIENCY OF THE ACTUATOR

5.1 The Solution of the Coupled Thermomechanical Problem

Recall that the heat flux quantity q in the first term of Eq.(3.17) needs to be specified from the interface conditions of the SMA with P/N. With the symmetry in the temperature field given by Eq.(4.13), it is sufficient to derive the heat flux q(defined first in Eq.(3.15)) either from Eq.(4.10) or (4.11) respectively, with the help of the second of Eq.(2.20) and Eq.(4.3). It is

$$q = -\kappa_p \frac{\partial T_p}{\partial z}(\frac{d}{2}, t) + \alpha_p T(t) J(t) \ . \tag{5.1}$$

Eq.(3.17) reduces to

$$\frac{2}{d}\left[\kappa_p \frac{\partial T_p}{\partial z}(\frac{d}{2}, t) - \alpha_p T(t) J(t)\right] - 2h\left(\frac{1}{b} + \frac{1}{w}\right)(T(t) - T_0) + \rho J(t)^2 = \left\{ C(\xi) + \gamma(\sigma, T)\left[\sqrt{\rho_{sma}\frac{\partial \Delta u(\xi)}{\partial \xi}}\right]^{-1} \psi(\xi) + \right.$$

$$\left. [\alpha^{th}(\xi) T(t) + \gamma(\sigma, T)\left[\sqrt{\rho_{sma}\frac{\partial \Delta u(\xi)}{\partial \xi}}\right]^{-1} \beta(\xi, \sigma, T)] s(\xi, \sigma, T) \right\} \dot{T}(t) \ . \tag{5.2}$$

The evolution equations (2.11) and (3.10) for ξ and σ can be solved alongwith the above equation once the heat flux term, $-\kappa_p \frac{\partial T_p}{\partial z}(\frac{d}{2}, t)$, is known. This implies that a fourth equation is needed; it is Eq.(4.9)(Due to the symmetry in the temperature field, we shall only consider the equation for the P element).

In absence of a stress field(when only Eqs.(4.9) and (5.2) will remain, with $s(\xi, \sigma, T) = 0$ in the latter), the thermoelectromechanical problem reduces to the one addressed by Lagoudas and Ding(1995). They show that it is possible, due to the linearity of the thermal problem in the P material, to derive an integro-differential equation solely in terms of the temperature of the SMA; the derived equation does not involve the temperature field of the P/N elements. They solved the equation by the finite difference scheme.

For the current problem, the methodology of Lagoudas and Ding(1995) is used to derive the following differential equation from Eqs.(4.9) and (5.2)

$$\frac{dT}{dt}(t) = S(t) - \nu_1 T(t) \ . \quad t > 0 \ , \tag{5.3}$$

where the temperature of the SMA, T(t), can be solved from the above equation(and with the initial condition, given by the first of Eq.(3.3)) once $S(t)$ is found from the solution of the integro-differential equation

$$\int_0^t G(t-\tau) S(\tau) d\tau + \mu(\xi, \sigma, T) S(t) + [\nu_2(t) - \mu(\xi, \sigma, T)\nu_1] \int_0^t e^{-\nu_1 (t-\tau)} S(\tau) d\tau$$

$$= F(t) - T_0 [\nu_2(t) - \mu(\xi, \sigma, T)\nu_1] e^{-\nu_1 t} \ . \tag{5.4}$$

The parameters $G(t)$, $\mu(\xi, \sigma, T)$, $\nu_2(t)$, ν_1 and $F(t)$ are given in the Appendix. Note that the coupling parameter $\gamma(\sigma, T)$ enters into Eq.(5.4) through the expression for $\mu(\xi, \sigma, T)$(see the third of Eq.(A.11) in the Appendix).

To summarise, Eqs.(2.11), (3.10) and (5.3) correspond to the evolution equation for the martensitic volume fraction, the conservation of linear momentum and the conservation of energy respectively. This system of first-order nonlinear ordinary differential equations alongwith the initial conditions given by Eqs.(3.3) and (3.13) and supplemented by Eq.(5.4) need to be solved for ξ, σ and T. The computational procedure is given in Sec 6.1.

5.2 Energy Conversion Efficiency of the Actuator

Before we move into the numerical scheme, it is desirable to characterize the performance of the thermoelectric SMA actuator. Normally, two different measures are used(Giurgiutiu *et.al.*,1995). These are:

(a) The energy output per unit volume of the active material which is stored in the actuated structure(the spring in our case) during the transformation of the SMA from martensite into austenite during heating. If the transformation starts at $t = t_0$, the energy stored during the transformation is given by

$$W^{act}(t) = \frac{bd}{w}\frac{1}{2k_s}\left[\sigma^2(t) - \sigma^2(t_0)\right] \ . \tag{5.5}$$

In case of a very compliant spring(i.e.implying a constant load boundary condition) with some initial stress, Eq.(5.5) is the work done per unit volume of the active material in displacing a constant load during the $M \rightarrow A$ transformation by heating.

(b) The associated energy conversion efficiency in converting the electrical energy input to the actuator into the energy stored in the spring during the $M \rightarrow A$ transformation. This is defined as

$$\eta(t) = \frac{W^{act}(t)}{W^e(t) - W^e(t_0)} \ , \tag{5.6}$$

where we define $W^e(t)$ as the electrical energy input per unit volume of the P/SMA/N assembly. It is given as

$$W^e(t) = \frac{1}{V}\int_0^t \int_V \boldsymbol{e}.\boldsymbol{j}\ dV d\tau \ , \tag{5.7}$$

where V is the volume of the P/SMA/N assembly. Using Eq.(2.21), the assumption $\nabla\mu = 0$ in the P/SMA/N and the last of Eq.(2.23), Eq.(5.7) becomes

$$W^e(t) = \frac{W^e_{sma}(t)V_{sma} + 2W^e_p(t)V_p}{V_{sma} + 2V_p} = \frac{W^e_{sma}(t)d + 2W^e_p(t)d_p}{d + 2d_p} \ , \tag{5.8}$$

where

$$W^e_{sma}(t) = \rho\int_0^t J^2(\tau)d\tau \ \text{ and } \ W^e_p(t) = \left[\frac{\alpha_p}{d_p}\int_0^t (T_0 - T(\tau))J(\tau)d\tau + \rho_p\int_0^t J^2(\tau)d\tau\right] \ . \tag{5.9}$$

At this point, we note that a thermoelectric device has been historically used as a refrigerator and to characterize its performance, the definition of "Coefficient of Performance"(COP)(Nag,1981) has been used. We shall now provide a point of contact between the notion of actuator efficiency and the COP of a thermoelectric device.

Whenever a thermoelectric device has been used as a refrigerator, its steady state "cooling" capability has been of interest and the COP has been defined in that context. In our case, it is the transient heat transfer that we are interested in; moreover the thermoelectric device is not only being used as a refrigerator but also as a heat pump. As we compute the efficiency of the actuator when the device is being used as a heat pump, we shall define the COP in the context of transient heating only. The COP is defined as

$$COP(t) = \frac{M_{sma}[Q(t) - Q(t_0)]}{W_e(t) - W_e(t_0)} , \tag{5.10}$$

where M_{sma} is the mass of the SMA layer and $Q(t)$ is the specific heat input(heat input per unit mass) into the SMA(defined in Eq.(5.11)). The numerator in the above equation represents the total thermal energy brought into the SMA layer at a temperature $T(t)$(with the heat sinks at T_0) during the transformation. $Q(t)$ is

$$Q(t) = \int_0^t \dot{Q}(\tau) d\tau , \tag{5.11}$$

where $\dot{Q}(t)$ follows from the right hand side of Eq.(3.17) as

$$\dot{Q}(t) = \frac{1}{\rho_{sma}} \left\{ C(\xi) + \gamma(\sigma, T) \left[\sqrt{\rho_{sma} \frac{\partial \Delta u(\xi)}{\partial \xi}} \right]^{-1} \psi(\xi) + \right.$$
$$\left. \left[\alpha^{th}(\xi) T(t) + \gamma(\sigma, T) \left[\sqrt{\rho_{sma} \frac{\partial \Delta u(\xi)}{\partial \xi}} \right]^{-1} \beta(\xi, \sigma, T) \right] s(\xi, \sigma, T) \right\} \dot{T}(t) . \tag{5.12}$$

The COP of a corresponding Carnot heat pump(i.e. the maximum attainable COP) is

$$COP_{carnot}(t) = \left[1 - \frac{T_0}{T(t)} \right]^{-1} . \tag{5.13}$$

With Eqs.(5.10) and (5.13), we can write Eq.(5.6) as

$$\eta(t) = \frac{W^{act}(t)}{M_{sma}[Q(t) - Q(t_0)]} \times \frac{COP(t)}{COP_{carnot}(t)} \times COP_{carnot}(t) . \tag{5.14}$$

Recognizing $\frac{W^{act}(t)}{M_{sma}[Q(t)-Q(t_0)]} = \eta_{sma}(t)$ as the efficiency by which the SMA layer converts heat into work and $\frac{COP(t)}{COP_{carnot}(t)} = COP_{rel}(t)$ as the COP of the thermoelectric device relative to a Carnot device, we then have

$$\eta(t) = \eta_{sma}(t) \times COP_{rel}(t) \times COP_{carnot}(t) . \tag{5.15}$$

In addition, it is reasonable to identify $\eta_{sma}(t) \times COP_{carnot}(t) = \eta_{carnot}(t)$ as the efficiency of the SMA layer when operated with a Carnot heat pump. Thus

$$\eta(t) = \eta_{carnot}(t) \times COP_{rel}(t) \; . \tag{5.16}$$

Therefore, $\eta_{carnot}(t)$ is the maximum attainable efficiency of the actuator whereas the efficiency, $\eta(t)$, of the "real" actuator is controlled by the $COP_{rel}(t)$ of the thermoelectric device.

5.3 Resume of the Nondimensionalized Solution

While the theoretical development was based on dimensional quantities, it is preferable to present the numerical results in a non-dimensional form. We thus obtain the nondimensional counterparts of physical quantities by the application of the Buckingham π theorem(Buckingham,1914), which are listed below. Note that for the thermoelectric problem, the relevant nondimensional groups were originally introduced by Bhattacharyya *et.al.*(1995).

Normalized absolute temperature: $\bar{T} = \dfrac{T}{T_0} - 1$,

Normalized stress: $\bar{\sigma} = \dfrac{\sigma}{E_M}$, Normalized time: $\bar{t} = t\left(\dfrac{C_p d_p^2}{\kappa_p}\right)^{-1}$,

Normalized convection coefficient: $\bar{h} = 2h\left(\dfrac{1}{b} + \dfrac{1}{w}\right)\dfrac{d_p^2}{\kappa_p}$, Normalized current: $\bar{J} = Jd_p\sqrt{\dfrac{\rho_p}{\kappa_p T_0}}$,

Normalized Seebeck coefficient: $\bar{\alpha}_p = \alpha_p\sqrt{\dfrac{T_0}{\kappa_p \rho_p}}$, Normalized coefficient of thermal expansion: $\bar{\alpha} = \alpha T_0$,

Normalized stress influence coefficient: $\bar{D} = \dfrac{D}{E_M/T_0}$, Thermomechanical Coupling Coefficient: $\bar{E}_{TC} = \dfrac{E}{T_0 C_p}$,

Normalized Spring Stiffness: $\bar{k}_s = \dfrac{k_s}{E_M w}$, Normalized initial stress: $\bar{\sigma}(0) = \dfrac{\sigma(0)}{E_M}$,

Relative Heat capacity of SMA: $\bar{C} = \dfrac{C}{C_p}$, Relative resistivity of SMA: $\bar{\rho} = \dfrac{\rho}{\rho_p}$,

Relative Young's modulus of SMA: $\bar{E} = \dfrac{E}{E_M}$,

Relative dimensions of the SMA and the P/N: $\bar{d} = \dfrac{d}{w}$, $\bar{b} = \dfrac{b}{w}$, $\bar{d}_p = \dfrac{d_p}{w}$. (5.17)

Using the nondimensional groups listed in Eq.(5.17), we present a resume of the final set of equations and the associated initial conditions, all in a nondimensionalised form. Eq.(3.10) for the conservation of linear momentum in the SMA reduces to

$$\dot{\bar{\sigma}}(\bar{t}) = \bar{s}(\xi, \bar{\sigma}, \bar{T})\dot{\bar{T}}(\bar{t}) \; , \tag{5.18}$$

where

$$\bar{s}(\xi, \bar{\sigma}, \bar{T}) = -\frac{\bar{E}_T(\xi, \bar{\sigma}, \bar{T})\bar{\alpha}_T(\xi, \bar{\sigma}, \bar{T})}{\frac{2\bar{V}_{sma}\bar{E}_T(\xi,\bar{\sigma},\bar{T})}{\bar{k}_s} + 1} \; , \tag{5.19}$$

where $\bar{E}_T(\xi,\bar{\sigma},\bar{T}) = E_T(\xi,\sigma,T)/E_M$, $\bar{\alpha}_T(\xi,\bar{\sigma},\bar{T}) = T_0\alpha_T(\xi,\sigma,T)$ and the normalized volume of the SMA is $\bar{V}_{sma} = \bar{b}\bar{d}$. Eq.(2.11) corresponding to the evolution equation for the volume fraction of martensite becomes

$$\dot{\xi} = \bar{\psi}(\xi)\dot{\bar{T}} + \bar{\beta}(\xi,\bar{\sigma},\bar{T})\dot{\bar{\sigma}} \ , \tag{5.20}$$

where

$$\bar{\psi}(\xi) = T_0\left[\sqrt{\rho_{sma}\frac{\partial\Delta u(\xi)}{\partial\xi}}\right]^{-1}\psi(\xi) \quad \text{and} \quad \bar{\beta}(\xi,\bar{\sigma},\bar{T}) = E_M\left[\sqrt{\rho_{sma}\frac{\partial\Delta u(\xi)}{\partial\xi}}\right]^{-1}\beta(\xi,\sigma,T) \ , \tag{5.21}$$

where the time derivatives in Eq.(5.20) are with respect to the nondimensional time, $\bar{t}$. Finally, Eq.(5.3) for the conservation of energy in the SMA reduces to

$$\frac{d\bar{T}}{d\bar{t}}(\bar{t}) = \bar{S}(\bar{t}) - \bar{\nu}_1[1+\bar{T}(\bar{t})] \ , \quad \bar{t} > 0 \ . \tag{5.22}$$

where $\bar{S}(\bar{t}) = \frac{C_p d_p^2}{\kappa_p T_0}S(t)$ and $\bar{\nu}_1$ is given in Eqs.(A.12) of the Appendix. The solution to the above differential equation can be found once the parameter $\bar{S}(\bar{t})$ is solved from the nondimensionalised version of Eq.(5.4), given as

$$\int_0^{\bar{t}} \bar{G}(\bar{t}-\bar{\tau})\bar{S}(\bar{\tau})d\bar{\tau} + \bar{\mu}(\xi,\bar{\sigma},\bar{T})\bar{S}(\bar{t}) + \left[\bar{\nu}_2(\bar{t}) - \bar{\mu}(\xi,\bar{\sigma},\bar{T})\bar{\nu}_1\right]\int_0^{\bar{t}} e^{-\bar{\nu}_1(\bar{t}-\bar{\tau})}\bar{S}(\bar{\tau})d\bar{\tau}$$
$$= \bar{F}(\bar{t}) - \left[\bar{\nu}_2(\bar{t}) - \bar{\mu}(\xi,\bar{\sigma},\bar{T})\bar{\nu}_1\right]e^{-\bar{\nu}_1\bar{t}} \ . \tag{5.23}$$

The parameters $\bar{G}(\bar{t})$, $\bar{\mu}(\xi,\bar{\sigma},\bar{T})$, $\bar{\nu}_2(\bar{t})$, $\bar{\nu}_1$ and $\bar{F}(\bar{t})$ are given in Eqs.(A.12) of the Appendix. The initial conditions for the nondimensional stress, the martensitic volume fraction and the nondimensional temperature, follow from Eqs.(3.3) and (3.13), as

$$\bar{\sigma}(0) = \frac{\bar{\delta}_0}{\frac{\bar{V}_{sma}}{k_s} + \frac{1}{2\bar{E}(0)}} \ , \ \xi(0) = \xi_0 \ , \ \bar{T}(0) = 0 \ . \tag{5.24}$$

The nondimensional energy stored during the transformation follows from Eq.(5.5) as

$$\bar{W}^{act}(\bar{t}) = \frac{\bar{V}_{sma}}{2\bar{k}_s}\left[\bar{\sigma}^2(\bar{t}) - \bar{\sigma}^2(\bar{t}_0)\right] \ . \tag{5.25}$$

The energy efficiency(see Eq.(5.16)) is intrinsically nondimensional, therefore

$$\bar{\eta}(\bar{t}) = \eta(t) \ . \tag{5.26}$$

Eqs.(5.18)-(5.26) constitute the nondimensionalised solution.

5.4 Thermomechanical Coupling

Before the issue of thermomechanical coupling during the phase transformation is addressed, we list some typical parameters for a Ni-Ti SMA. These are(Jackson *et.al.*,1972)

$$
\begin{aligned}
&M_s^0 = 23^0C \ , \ M_f^0 = 1^0C \ , \ A_s^0 = 29^0C \ , \ A_f^0 = 51^0C \ , \\
&H_a = 0.148 \ J/mm^3 \ , \ H = 8\% \ , \ s_p = 3.5 \ , \\
&E_A = 70 \times 10^3 \ MPa \ , \ E_M = 30 \times 10^3 \ MPa \ , \ \nu_A = \nu_M = 1/3 \ , \\
&\alpha_A = 11 \times 10^{-6}/^0C \ , \ \alpha_M = 6.6 \times 10^{-6}/^0C \ ,
\end{aligned} \tag{5.27}
$$

where M_s^0 and M_f^0 are the stress-free martensitic start and finish temperatures, A_s^0 and A_f^0 are the austenite start and finish temperatures, H_a is the magnitude of the latent heat, H is the maximum uniaxial inelastic transformation strain and s_p is the standard deviation of the normal distribution $p(T)$ defined in Eq.(A.6) of the Appendix. E_i and ν_i are the Young's modulus and the Poisson's ratio of the ith phase(i=A,M). With these values, we compute

$$
D = 6.187 \ MPa/^0C \ \text{ and } \ Y = 6.93 \ MPa \ , \tag{5.28}
$$

from Eq.(A.10) in the Appendix. The thermoelectric properties of the SMA and the P element are summarized in the table below. Note that the thermoelectric properties of the N element will follow from Eq.(4.12).

	$\alpha(V/K)$	κ(J/(mm.s-K)	$\rho(\Omega$-mm)	C $(J/(mm^3 - K)$)
SMA	1.2×10^{-5}	2.2×10^{-2}	6.3242×10^{-4}	2.12×10^{-3}
P	2.15×10^{-4}	1.63×10^{-3}	1.15×10^{-2}	4.35×10^{-3}

Table 1. Material Constants of SMA and Semiconductor elements.

The geometric parameters are assumed to be

$$
b = w = 4 \text{ mm} \ , \ d_p = 2 \text{ mm} \ , \ d = 0.5 \text{ mm} \ . \tag{5.29}
$$

The convection coefficient is taken as

$$
h = 1 \times 10^{-6} J/(mm^2 sK)^{-1} \ . \tag{5.30}
$$

The above value of h was found suitable by Bhattacharyya *et.al.*(1995) to model free convection conditions. The initial values of the stress, martensitic volume fraction and the temperature are taken as

$$
\sigma(0) = 0 \ , \ \xi(0) = 1 \ , \ T(0) = 297^0 \ K \ . \tag{5.31}
$$

The spring stiffness and the current density are chosen as

$$
k_s = 3 \ KN/mm \ , \ J = 3 \ Amps/mm^2 \ . \tag{5.32}
$$

Based on the above, we now give the nondimensional parameters. Note that among those listed in Eq.(5.17), the evolution of the nondimensional temperature and the stress, $\bar{T}$ and $\bar{\sigma}$, with the nondimensional time, $\bar{t}$, are of interest. The paremeters $\bar{\alpha}$, $\bar{E}_{TC}$ and $\bar{E}$ depend on the state variable, ξ and hence will follow from the solution. The remaining nondimensional parameters therefore are

$$\bar{h} = 2.454 \times 10^{-3} \ , \ \bar{\alpha}_p = 0.856 \ , \ \bar{D} = 6.125 \times 10^{-2} \ , \ \bar{C} = 0.487 \ ,$$
$$\bar{\rho} = 0.055 \ , \ \bar{b} = 1 \ , \ \bar{d}_p = 0.5 \ , \tag{5.33}$$

whereas

$$\bar{J} = 0.925 \ , \ \bar{\sigma}(0) = 0 \ , \ \bar{k}_s = 0.025 \ , \ \bar{d} = 0.125 \ . \tag{5.34}$$

Among the nondimensional parameters, only those in Eq.(5.34) will be treated as variable parameters in the numerical studies; hence, their numerical values will be mentioned in the inset of the figures. The computational scheme based on which the numerical results were generated has been discussed in detail in Sec.6.1.

In order to understand the thermomechanical coupling in the heat conduction equation Eqs.(5.22)-(5.23), it is perhaps more useful to start from the nondimensional form of Eq.(2.15)(from which Eqs.(5.22)-(5.23)) were derived). It is

$$-\overline{\nabla}.\overline{q} + \bar{r} = \frac{\bar{C}}{\bar{E}_{TC}}\dot{\bar{T}} + (1+\bar{T})\bar{\alpha}^{th} : \dot{\bar{\sigma}} + \bar{\gamma}\dot{\xi} \ , \tag{5.35}$$

where among the nondimensional parameters involved in the above equation, those not listed in Eq.(5.17) are $\overline{\nabla}.\overline{q} = \frac{C_p d_p^2}{E_M \kappa_p}\nabla.q$, $\bar{r} = \frac{C_p d_p^2}{E_M \kappa_p} r$ and $\bar{\gamma} = \gamma/E_M$; note that the rate terms in Eq.(5.35) are with respect to the nondimensional time. Our intention here is to uncover the effect of the coupling term $\bar{\gamma}\dot{\xi}$. Towards that end, we look at the evolution of $\bar{T}$ vs. $\bar{t}$ and $\bar{\sigma}$ vs. $\bar{t}$ given in Fig.2a and Fig.2b respectively for two cases: (a) the line 1 corresponds to omitting the term, $\bar{\gamma}\dot{\xi}$ from Eq.(5.35) and (b) the line 2 corresponds to retaining the term $\bar{\gamma}\dot{\xi}$. In both cases, the SMA, starting from an initially fully martensitic condition, is heated until it is fully converted into austenite($\xi = 0$), following which the current direction is reversed to cool the SMA layer until the austenite fully converts to martensite. The effect of the phase transformation is seen to slow the heating and the cooling process.

With the material parameters given in the beginning of this section, it can be shown that $\bar{\gamma} = \gamma/E_M = (T\sigma\Delta\alpha + \rho\Delta s_0 T - \Pi)/E_M \approx -H_a/E_M$ where H_a is the magnitude of the latent heat of transformation($H_a > 0$). Thus, the term $\bar{\gamma}\dot{\xi}$(or $-\frac{H_a}{E_M}\dot{\xi}$) represents the latent heat exchanged during a phase transformation. When $\dot{\xi} < 0$(during heating), this term acts as a heat sink and indicates the endothermic nature of the $M \rightarrow A$ transformation; the effect is to slow the temperature increase, evident from a comparison of the heating portion of curve 2 with that of curve 1 in Fig.2a. During the $A \rightarrow M$ transformation upon cooling, the term $-\frac{H_a}{E_M}\dot{\xi}$ acts as a heat source and is indicative of the exothermic nature of the $A \rightarrow M$ phase transformation. This results in a slower

cooling process; compare cooling portions of curves 2 and 1. These trends in the evolution rate are also reflected in the evolution of $\bar{\sigma}$, in Fig.2b.

We also examine the issue by estimating the relative magnitudes of the terms on the right hand side of Eq.(5.35). As the SMA is heated from $\xi = 1$ to 0(refer the line 2 in Figs.2a and b), the change in $\bar{T}$ and $\bar{\sigma}$ are approximately $\Delta\bar{T} = 0.22$ and $\Delta\bar{\sigma} = 7.5\times10^{-3}$ and the change in ξ is $\Delta\xi = -1$. Over the time range that this transformation has taken place, the cumulative change in the terms on the right hand side of Eq.(5.35), will be of the order of $\frac{\bar{C}}{E_{TC}}\Delta\bar{T}$, $(1+\bar{T})\bar{\alpha}^{th}\Delta\bar{\sigma}$ and $\bar{\gamma}\Delta\bar{\xi}$, respectively; these are estimated to be 1.979×10^{-3}, 2.99×10^{-5} and 4.93×10^{-3}, respectively. It is seen then that the thermoelastic coupling term(the second term in the list) is relatively very small whereas the heat capacity term(the first term) and the coupling term due to phase transformation(the last term) are of the same order of magnitude, with the latter being the more predominant one. This suggests that while the thermoelastic coupling term may still be omitted, the one due to the phase transformation, $\bar{\gamma}\dot{\bar{\xi}}$, must be retained. This has not always been the practice in the literature where both terms have been omitted to enable decoupling of the heat conduction equation from the mechanical problem for numerical simplicity(Brinson,1994,Oberaigner,1995).

Before closing, we further assess the relative importance of the stress rate term and the temperature rate term constituting $\dot{\xi}$ in Eq.(5.20). The ratio of the net evolution of each term is of the order of $-E_M\Delta\bar{\sigma}/(T_0 D\Delta\bar{T})$; this ratio follows from Eqs.(5.21), (91b) and the discussion in Sec.A of the Appendix. Its numerical value turns out to be around -0.56. Therefore, the temperature rate term and the stress rate term are of the same order. The combined effect of both terms is responsible for the thermomechanical coupling during phase transformation.

6. THE COMPUTATIONAL SCHEME AND PARAMETRIC STUDIES

6.1 The Computational Scheme

The system of evolution equations (5.18), (5.20) and (5.22) will be solved for $\bar{\sigma}$, ξ and $\bar{T}$ incrementally in time, using the fourth order Runge Kutta method in a nonlinear manner. However, since the coefficients of these equations themselves depend on $\bar{\sigma}$, ξ and $\bar{T}$, an iterative procedure additionally is required at every time step. Thermomechanically coupled problems have been addressed in the past, see Allen(1991) and Armero and Simo(1991). For our specific problem, we outline the numerical approach adopted. We shall first discuss the implementation of the Runge-Kutta method and then the iterative scheme.

If $\Delta\bar{t}$ is the duration of a time increment, we define

$$\xi_n = \xi(n\Delta\bar{t}), \bar{\sigma}_n = \bar{\sigma}(n\Delta\bar{t}) \text{ and } \bar{T}_n = \bar{T}(n\Delta\bar{t}) \ , \tag{6.1}$$

for each positive integer n; given the values $\xi_{n-1}, \bar{\sigma}_{n-1}$ and $\bar{T}_{n-1}$ at the (n-1)th time step, we need to compute the values $\xi_n, \bar{\sigma}_n$ and $\bar{T}_n$ at the nth time step. This is done by first writing Eq.(5.18)

as

$$\bar{\sigma}_n - \bar{\sigma}_{n-1} = \bar{s}(\xi^*, \bar{\sigma}^*, \bar{T}^*)(\bar{T}_n - \bar{T}_{n-1}) \ , \tag{6.2}$$

and Eq.(5.20) as

$$\xi_n - \xi_{n-1} = \bar{\psi}(\xi^*)(\bar{T}_n - \bar{T}_{n-1}) + \bar{\beta}(\xi^*, \bar{\sigma}^*, \bar{T}^*)(\bar{\sigma}_n - \bar{\sigma}_{n-1}) \ , \tag{6.3}$$

where initially, we assign

$$\xi^* = \xi_{n-1} \quad , \quad \sigma^* = \sigma_{n-1} \quad \text{and} \quad T^* = T_{n-1} \ . \tag{6.4}$$

The temperature increment is found by integrating Eq.(5.22) by the fourth-order Runge Kutta method(Numerical Recipes,1986); this approach is somewhat more accurate than the finite difference scheme used by Lagoudas and Ding(1995). Thus

$$\bar{T}_n - \bar{T}_{n-1} = \frac{k_1}{6} + \frac{k_2}{3} + \frac{k_3}{3} + \frac{k_4}{6} \ , \tag{6.5}$$

where

$$\begin{aligned}
k_1 &= \Delta\bar{t}\left[\bar{S}(\bar{t}_{n-1}) - \bar{\nu}_1 - \bar{\nu}_1\bar{T}(\bar{t}_{n-1})\right] \ , \\
k_2 &= \Delta\bar{t}\left[\bar{S}(\bar{t}_{n-1} + \frac{\Delta\bar{t}}{2}) - \bar{\nu}_1 - \bar{\nu}_1\bar{T}(\bar{t}_{n-1}) - \bar{\nu}_1\frac{k_1}{2}\right] \ , \\
k_3 &= \Delta\bar{t}\left[\bar{S}(\bar{t}_{n-1} + \frac{\Delta\bar{t}}{2}) - \bar{\nu}_1 - \bar{\nu}_1\bar{T}(\bar{t}_{n-1}) - \bar{\nu}_1\frac{k_2}{2}\right] \ , \\
k_4 &= \Delta\bar{t}\left[\bar{S}(\bar{t}_n) - \bar{\nu}_1 - \bar{\nu}_1\bar{T}(\bar{t}_{n-1}) - \bar{\nu}_1 k_3\right] \ ,
\end{aligned}$$

$\bar{S}(\bar{t})$ is given by

$$\bar{S}(\bar{t}) = \bar{S}_D\left[\int_{\bar{t}_{n-1}}^{\bar{t}} \left[\bar{G}(\bar{t}-\bar{\tau}) + \left[\bar{\nu}_2(t) - \bar{\mu}(\xi^*, \bar{\sigma}^*, \bar{T}^*)\bar{\nu}_1\right] e^{-\bar{\nu}_1\bar{t}}\right] d\bar{\tau}\right]^{-1} \ , \tag{6.6}$$

$$\begin{aligned}
\bar{S}_D = \bar{F}_n &- [\bar{\nu}_2(\bar{t}) - \bar{\mu}(\xi^*, \bar{\sigma}^*, \bar{T}^*)\bar{\nu}_1]e^{-\bar{\nu}_1\bar{t}} \\
&- \sum_{k=1}^{n-1} \bar{S}_k \int_{(k-1)\Delta\bar{t}}^{k\Delta\bar{t}} \left[\bar{G}(\bar{t}-\bar{\tau}) + \left[\bar{\nu}_2\bar{t} - \bar{\mu}(\xi^*, \bar{\sigma}^*, \bar{T}^*)\bar{\nu}_1\right]\right] e^{-\bar{\nu}_1\bar{t}} d\bar{\tau} \ .
\end{aligned}$$

and

$$\bar{F}_n = \bar{F}(n\Delta\bar{t}) \ , \bar{S}_n = \bar{S}_n(n\Delta\bar{t}) \ , \bar{G}_n = \frac{1}{\Delta\bar{t}}\int_{(n-1)\Delta\bar{t}}^{n\Delta\bar{t}} \bar{G}(\bar{t}) \, d\bar{t} \ , \ \bar{H}_n = \bar{H}(n\Delta\bar{t}) \ . \tag{6.7}$$

Note that we solve Eq.(6.5) for $\bar{T}_n$ and thereby Eqs.(6.2), followed by (6.3). We now have the first set of trial values for $\bar{\sigma}_n$, ξ_n and $\bar{T}_n$. If the difference $|\bar{T}_n - \bar{T}^*| > \delta$(where δ is a small number), then we set ξ^*, $\bar{\sigma}^*$ and $\bar{T}^*$ equal to the newly computed updated values and then recalculate a second set

of trial values from Eqs.(6.5), (6.2) and (6.3). This procedure is repeated until $|\bar{T}_n - \bar{T}^*| < \delta$; the convergence for ξ_n, $\bar{\sigma}_n$ and $\bar{T}_n$ is then achieved. We mention at this point that while the convergence criterion has been based solely on $\bar{T}_n$, our numerical computations confirm excellent simultaneous convergence for ξ and $\bar{\sigma}_n$.

6.2 Parametric Studies

We recall that in Sec.5.4 on "The Thermomechanical Coupling", it was mentioned that $\bar{\alpha}$, $\bar{E}_{TC}$ and $\bar{E}$ depend on the state variables ξ and will follow from the solution of the problem; the parameters are given in Eq.(5.33) and will be assumed to remain unchanged in the rest of the parametric study. Thus, the influence of the parameters, $\bar{J}$, $\bar{\sigma}(0)$, $\bar{k}_s$ and $\bar{d}$ on $\bar{T}$ and $\bar{\sigma}$ as a function of $\bar{t}$ is of interest. While the parametric study will be primarily based on non-dimensional parameters, we shall end with a sample case based on dimensional parameters in order to get a feel for the physical quantities involved. We note at this point that the frequency of cycling is dependent on the amount of austenite that is allowed to form(or the amount of martensite that remains) at the end of the heating cycle. We shall thus introduce the parameter ξ_{res} to denote the residual martensite volume fraction at the end of the heating cycle and assume $\xi_{res} = 0.8$ in the following analysis.

Initially, we shall investigate the influence of the parameters $\bar{k}_s$ and $\bar{\sigma}(0)$; the former corresponds to the stiffness of the actuator controlled structure and the latter is the initial stress exerted on the actuator due to an initial structural deformation. We shall fix $\bar{J} = 0.925$ and $\bar{d} = 0.125$(the values initially assumed in Eq.(5.34)) and the evolution of $\bar{T}$ and $\bar{\sigma}$ shall be studied for a range of $\bar{k}_s$ and $\bar{\sigma}(0)$.

In order to simulate a constant load and a variable load boundary condition, we consider two different spring stiffnesses, $\bar{k}_s = 8.3\times10^{-7}$ and 2.5×10^{-2}. Fig.3a gives the nondimensional temperature for both stiffnesses with the same initial nondimensional stress, $\bar{\sigma}(0) = 1.67 \times 10^{-3}$(corresponding to 50 MPa with the dimensional parameters given in Sec.5.4). It is seen from Fig.3b that the nondimensional stress(and by implication, the dimensional one) does not change during the course of the transformation for the more compliant spring; the value of $\bar{k}_s = 8.3 \times 10^{-7}$ is thus sufficient to simulate a constant load boundary condition.

We now return to Fig.3a. It is seen that the two curves for $\bar{T}$ at the two different spring stiffnesses are virtually indistinguishable up to a certain point, following which these separate. The onset of the $M \rightarrow A$ transformation is almost identical in both cases. A slight difference occurs because while both start out with an identical stress state, the thermal expansion of the SMA on heating(and prior to the onset of the $M \rightarrow A$ transformation) alters the stress state differently in the two cases. However, since the thermal strains are usually very small, the stress states in both cases are only marginally different. Recalling that the transformation temperatures are highly sensitive to

the magnitude of the uniaxial stress(increasing with stress and vice-versa), "almost" identical stress states imply "almost" identical transformation temperatures. This implies that the onset is almost identical in both cases. However, with the contraction due to phase transformation(substantial in comparison to the thermal expansion), the subsequent evolution of the stress in the two cases is substantially different, as is obvious from Fig.3b. The increasing stress state in the stiffer spring raises the transformation finish temperature and thus delays the completion of the transformation, in comparison to the compliant spring; hence with a stiffer spring, the frequency of cycling will always be lower than the one with a more compliant spring(with the same initial stress in both cases).

The nondimensional energy output $\bar{W}^{act}$ and the energy conversion efficiency η defined in Eqs.(5.25) and (5.26) are computed at the end of the $M \rightarrow A$ transformation(corresponding to $\xi_{res} = 0.8$). Their values at various initial stress levels and spring stiffnesses have been shown in Figs.4a and 4b(in these figures, the computed data points have been indicated with open circles and then connected by straight lines; such a procedure has been also adopted in Figs.4c through 7). It is seen in Fig.4a that at a given initial stress level, an increasing spring stiffness leads to a greater work output. This can be anticipated. With a higher spring stiffness, the stress rate will also be higher. Thus at the end of the transformation, while identical inelastic strains are recovered in all cases, the stress corresponding to a stiffer spring will be higher and thus will lead to a greater work output. However, the energy conversion efficiency(see Fig.4b) decreases with a stiffer spring at a given stress level; this physically happens because with a higher stress rate, the material needs to go to higher temperatures to complete the transformation leading to the enhanced consumption of electrical energy. For comparison, we also give the corresponding values of η_{carnot}, defined prior to Eq.(5.16). It is seen that the maximum achievable efficiency is an order of magnitude higher than the real efficiency η. This implies(see Eq.(5.16)) that the COP of a thermoelectric heat pump is an order of magnitude less efficient compared to a Carnot thermoelectric heat pump.

At this point, it is desirable to compare these performance measures to other commercially available actuators. Giurgiutiu *et.al.*(1995) have reported a comparative study of ferroelectric, electrostrictive and magnetostrictive actuators. The energy output per unit volume is the highest for an electrostrictive actuator, $W^{act} = 11.913\ J/m^3$, whereas a magnetostrictive actuator has the highest reported energy conversion efficiency of $\eta = 67.1$ %. For the thermoelectric SMA actuator, we find that $\bar{W}^{act} = 2.884 \times 10^{-5}$, implying that $W^{act} = \bar{W}^{act} E_M = 86.52 \times 10^4\ J/m^3$, and $\eta = 1.35\%$, attainable in a test case corresponding to the parameters used to generate the full transformation($\xi_{res} = 0$) cyclic response curve(line 2) in Fig.2. Therefore, the SMA thermoelectric actuator, in comparison with the actuators studied by Giurgiutiu *et.al.*(1995), has a very high energy output per unit volume of active material(four orders of magnitude) and a very low energy conversion efficiency. These results can be anticipated since SMAs have very high recoverable strains(assumed 8% in our case) compared to about 0.143% for the electrostrictive material(from

Table 3 of Giurgiutiu *et.al.*,1995); thus the specific energy output for the SMA actuator is expected to be considerably higher. On the other hand, a SMA relies on the conversion of heat into mechanical energy whereas electrostrictive and magnetostrictive materials convert electrical and magnetic energies directly into mechanical energy. Thermal energy being of a lower grade compared to electrical and magnetic energies, the conversion of the former into useful mechanical work is accomplished with a lower efficiency as compared to the conversion of the latter.

While it was instructive to compare the energy output and the energy conversion efficiency of the SMA actuator with that of other commercially available actuators, the key issue for SMA actuators is to address the question of actuator frequency. In the remaining part of the nondimensional parametric study, we shall confine ourselves to the issue of frequency response. We therefore turn to the nondimensional frequency of actuation, $\bar{\omega}$, depicted in Fig.5. If ω is the frequency of actuation(number of cycles per second), then $\bar{\omega} = \frac{C_p d_p^2}{\kappa_p}\omega$. It is seen that at both initial stress levels, the frequency decreases with increasing spring stiffness(this was first noted when discussing Fig.3a). In order to get an idea about the dimensional frequency, we choose a sample case; i.e. $\bar{k}_s = 0.025$ and $\sigma(0) = 3.33 \times 10^{-3}$, for which $\bar{\omega} = 13.9$ from Fig.5. The corresponding dimensional frequency with the parameters given in Sec.5.4 is then 1.3 Hz.

In Fig.6, we fix $\bar{\sigma}(0) = 3.33 \times 10^{-3}$ and the ratio $\bar{d}/\bar{k}_s = 5$. Bound by this condition, we study the influence on $\bar{\omega}$ due to a change in $\bar{d}$ and $\bar{k}_s$. This is done at two different levels of the current density, $\bar{J}$. It is seen that a decreasing thickness $\bar{d}$(and a consistent change in $\bar{k}_s$), at a given value of the current $\bar{J}$, leads to a higher nondimensional frequency, $\bar{\omega}$. Now let us examine the dimensional frequency, ω, for a test case: $\bar{J} = 1.23$ and $\bar{d} = 2.5 \times 10^{-3}$ for which $\bar{\omega} = 102.6$, from Fig.6. With the relevant parameters given in Sec.5.4, these nondimensional quantities translate to $\omega = 9.616$ Hz at $J = 4\ Amps/mm^2$, d = 10 μ. It can thus be concluded that very thin SMA actuators have relatively fast response. As an aside, we note that the two curves intersect each other around $\bar{d} > 0.11$. This is because for thicker SMAs during cooling, the Joule heating begins to dominate over the Peltier effect when the current density exceeds a certain critical value(Lagoudas and Ding,1995);thus the cooling rate decreases or the time needed to cool down to a certain temperature increases and reduces the frequency of actuation. When the SMA thickness is reduced below $\bar{d} \approx 0.11$, this critical value exceeds the normalized current densities shown in the figure. Thus below $\bar{d} = 0.11$, $\bar{\omega}$ increases as $\bar{J}$ increases from 0.925 to 1.23.

Until now, we have not discussed the influence of material parameters on the frequency. To be specific, it is well known that the hysteresis in the stress-free transformation temperatures in a NiTi SMA are highly sensitive to alloying elements(Jackson *et.al.*,1972) and thus, it is a parameter of interest. The influence of the hysteresis on the frequency is now studied.

Recall that the hysteresis in the stress-free transformation temperatures is responsible for the dissipation during a phase transformation in the SMA. In the constitutive theory for SMAs we have used here, a reference to the work of Boyd and Lagoudas(1995) shows that the term, $\int \Pi d\xi$,

represents the cumulative dissipation during the phase transformation and over a complete cycle of the $M \rightarrow A$ and $A \rightarrow M$ transformations, it is straightforward to show from Eq.(2.18) that the net dissipation is $2Y$; Y is thus a measure of dissipation. We shall now establish the link between the parameter Y and the transformation temperature hysteresis. For simplicity, we assume that the spread between the start and finish temperatures during both transformations is identical,i.e.

$$A_f^0 - A_s^0 = M_s^0 - M_f^0 \quad \rightarrow \quad A_s^0 - M_f^0 = A_f^0 - M_s^0 \ . \tag{6.8}$$

We now define the transformation temperature hysteresis as the parameter $\Delta T_{AM} = A_s^0 - M_f^0 = A_f^0 - M_s^0$, such that $A_s^0 = M_f^0 + \Delta T_{AM}$ and $A_f^0 = M_s^0 + \Delta T_{AM}$. With these definitions, we rewrite Y from the second of Eq.(A.10) in the Appendix as

$$Y = \frac{1}{2} HD \left[\int_{M_s^0}^{M_f^0} Tp(T)dT - \int_{M_s^0+\Delta T_{AM}}^{M_f^0+\Delta T_{AM}} Tp(T)dT \right] \ . \tag{6.9}$$

Notice that if $\Delta T_{AM} = 0$, then $Y = 0$; this implies that in absence of hysteresis, the dissipation vanishes. The above equation then links the measure of dissipation to the hysteresis in the transformation temperatures. With respect to the temperatures in Eq.(5.27), the first of Eq.(6.8) shows that $A_f^0 - A_s^0 = M_s^0 - M_f^0 = 22^0 C$ whereas $\Delta T_{AM} = 28^0 C$ from Eq.(5.27). For the parametric study, we keep the former fixed and change the hysteresis ΔT_{AM} in the range $20 \leq \Delta T_{AM} \leq 28$(reducing ΔT_{AM} below 20 raises issues regarding minor loops(Mayergoyz,1991), and is beyond the scope of this paper). It is seen from Fig.7 that a decrease in the hysteresis results in a substantial increase in frequency. With $\Delta T_{AM} = 20^0 C$, $\bar{\omega} = 143$; the corresponding dimensional frequency based on the dimensional parameters in Sec.5.4 is $\omega = 13.4$. If however we set $J = 6\ Amps/mm^2$, then we have $d_p = 1.33$ mm, $b = w = 2.67$ mm, $d = 6.67\mu$ and the dimensional frequency becomes $\omega = 30.15$ Hz; the evolution of the dimensional temperature and stress are shown in Fig.8.

We now return to Eq.(2.1) where the inertial effects were ignored and the conservation of linear momentum reduced to the equilibrium equation. We shall provide an estimate of these effects at the relatively high frequency of $\omega = 30.15$ Hz and show that the assumption made is indeed a reasonable one for the frequency range considered. To arrive at an estimate of the order of magnitude, we make the simplifying assumption that the accelaration, a, is constant and derive it from the displacement of the surface, $x = \frac{w}{2}$; thus $\frac{1}{2}at^2 = \epsilon\frac{w}{2}$. The inertial force, $M_{sma}a$, has to be compared with the actuation force, $\sigma(t)bd$. We then compute the ratio $M_{sma}a/\sigma(t)bd = 4\rho_{sma}\epsilon\omega^2 W^2 \sigma(t)^{-1}$ at the end of the first half of the first cycle(during the $M \rightarrow A$ transformation) where the actuation force attains its maximum. The ratio turns out to be 0.87 % for the case shown in Fig.8; neglecting inertial effects thus appears to be reasonable.

7. CONCLUSIONS

As a first step towards the design of a high frequency, high force, large strain SMA actuator, we have modeled in this work a thermoelectrically cooled thin SMA strip linear actuator. The

SMA undergoes cyclic phase transition between the martensitic and austenitic phases by alternate heating/cooling, achieved with the thermoelectric Peltier effect of a pair of P/N semiconductors. The effect of variable actuating load and constant load applied as boundary conditions on the SMA actuator have been considered. The thermomechanical boundary value problem involves strongly coupled thermal and mechanical fields. The evolution equations for the field variables are integrated using the fourth-order Runge Kutta method and the coupling between the fields is accounted for by implementing an interative scheme. The primary parameters of interest in this work are the frequency response and evolution of the variable load. The performance of the actuator is compared with various commercially available actuators based on energy conversion efficiencies and energy output per unit volume of active material. With reference to Fig.8, we conclude that thin layers of SMA about 6 μ thick, with a low transformation hysteresis and undergoing partial transformation, are potentially capable of delivering frequencies of the order of 30 Hz at peak stresses of about 145 Mpa.

ACKNOWLEDGEMENTS

The authors acknowledge the financial support of the Office of Naval Research, contract No. N 00014-94-1-0268, monitored by Dr. Roshdy Barsoum.

REFERENCES

1. Allen, D.H, Thermomechanical Coupling in Inelastic Solids, in *Review of Thermal Stresses*, Edited by Richard B. Hetnarski, Applied Mechanics Reviews, **44**, Nos.8-9, 361 (1991).

2. Armero, F. and Simo, J.C., A New Unconditionally Stable Fractional Step Method for Nonlinear Coupled Thermomechananical Problems, Sudam Report No.91-5, Stanford University (1991).

3. Bhattacharyya, A., Lagoudas, D.C., Wang, A. and Kinra, V.K., "On the Role of Thermoelectric Heat Transfer in the Design of SMA Actuators: Theoretical Modeling and Experiment",*Smart Mater. Struct.*, **4**, 252 (1995).

4. Bhattacharyya, A. and Lagoudas, D.C., A Stochastic Thermodynamic Model for the Gradual Thermal Transformation of SMA Polycrystals, *Journal of Smart Materials and Structures* (submitted) (1995).

5. Bo, Z. and Lagoudas, D.C., "Deformations and Thermal Response of Active Flexible Rods with Embedded SMA Actuators", *Smart Structures and Materials 1994: Smart Structures and Intelligent Systems*, Proceedings of the SPIE 1994 North American Conference on Smart Structures, Orlando, FA, **2190** (1994).

6. Boley, B.A. and Weiner, J.H.,"Theory of Thermal Stresses", Krieger Pub. Co., Florida (1960).

7. Boyd, J. and Lagoudas, D.C., "A Thermodynamic Constitutive Model for Shape Memory Materials. Part I: The Monolithic Shape Memory Alloy and Part II: The SMA Composite Material", *Int. J. Plasticity*(in press) (1995).

8. Brinson, L.C., Bekker and Hwang,S., "Temperature Induced Deformation in Shape Memory Alloys", in *Active Materials and Smart Structures*, Edited by: Anderson, G.L. and Lagoudas, D.C., 31^{st} Annual Technical Meeting of the Society of Engineering Science, **2427**, 234 (1995).

9. Buckingham, E., "On Physically Similar System Illustrations of the Use of Dynamical Equations", *Phys. Rev.*, **4**, 376 (1914).

10. Delaey, L., Krishnan, R.V., Tas,H. and Warlimont,H., "Thermoelasticity, Pseudoelasticity and the Memory Effects associated with Martensitic Transformations" Parts I-III *Journal of Materials Science*, 1521 (1974).

11. Domenciali, C.A., "Irreversible Thermodynamics of Thermoelectricity", *Reviews of Modern Physics*, **26**, No.2 , 237 (1954).

12. Giurgiutiu, V., Chaudhry, Z. and Rogers, C.,"Energy-Based Comparison of Solid-State Actuators", Technical Report, Center for Intelligent Material Systems and Structures, VPI-SU, Blacksburg, VA (1995).

13. Harman, T.C., and Honig, J.M., "Thermoelectric and Thermomagnetic Effects and Applications", Mc-Graw Hill Book Co., NY (1967).

14. Jackson, C.M., Wagner, H.J. and Wasilewski, R.J., "A report on 55-Nitinol – The Alloy with a Memory: Its Physical Metallurgy, Properties and Applications", Technology Untilization Office, NASA, Washington, D.C (1972).

15. Lagoudas, D.C., Bo, Z. and Bhattacharyya, A., "A Thermodynamic Constitutive Model for Gradual Phase Transformation of SMA Materials", Proceedings of the SPIE Conference, San Deigo, CA, 1996(accepted) (1996).

16. Lagoudas, D.C. and Ding, Z., "Modeling of Thermoelectric Heat Transfer in Shape Memory Alloy Actuators: Transient and Multiple Cycle Solutions",",*Int. J. Engng Sci.*, **33**, No.15, 2345 (1995).

17. Lagoudas, D.C. and Kinra, V.K., "Design of High Frequency SMA Actuators, Disclosure of Invention Tamus 803, Texas A&M University, College Station, TX 77843 (1993).

18. Liang, C. and Rogers, C.A., "One-Dimensional Thermomechanical Constitutive Relations for Shape Memory Materials", *Journal of Intelligent Materials Systems and Structures*, **1**, 207 (1990).

19. Liang, C. and Rogers, C.A., "The Multi-dimensional Constitutive Relations of Shape Memory Alloys", Proceedings, *AIAA 32nd Structures, Structural Dynamics and Materials Conference*, Baltimore, MD (1991).

20. Mayergoyz, I.D., "Mathematical Models of Hysteresis", Springer Verlag, 1983.

21. Melcor Educational Package, Melcor, Trenton, NJ (1992).

22. Nag, P.K.,"Engineering Thermodynamics", Tata McGraw-Hill, New Delhi, India (1981).

23. Numerical Recipes: The Art of Scientific Computing, Cambridge University Press, London (1986).

24. Oberaigner,E.R., Tanaka,K. and Fischer,F.D., "Investigation of the Damping Behavior of a Vibrating Shape Memory Alloy Rod using a Micromechanical Model", in *Mathematics and Control in Smart Structures*, Edited by V.V. Varadan, Proceedings of SPIE, 349 (1995).

25. Patoor, E.,Eberhardt, A. and Berveiller, M., "Potentiel Pseudoelastique et Plasticite de Transformation Martenistique dans les Mono-et Polycristaux Metalliques", *Acta Metallurgica*, **35**, No.11, 2779 (1987).

26. Pollock, D.D., "Thermocouples: Theory and Properties", CRC Press, Boson, MA (1991).

27. Sun, Q.P. and Hwang, K.C., "Micromechanics Modeling for the Constitutive Behavior of Polycrystalline Shape Memory Alloys-I. Derivation of General Relations", *J. Mech. Phys. Solids*, **41**, 1 (1993a).

28. Sun, Q.P. and Hwang, K.C., "Micromechanics Modeling for the Constitutive Behavior of Polycrystalline Shape Memory Alloys-I. Study of the Individual Phenomena", *J. Mech. Phys. Solids*, **41**, 19 (1993b).

29. Takagi, T., "A Concept of Intelligent Materials", *Journal of Intell. Mater. Sys. and Struct.*, **1**, 149 (1990).

30. Tanaka, K., "A Thermomechanical Sketch of Shape Memory Effect: One-Dimensional Tensile Behavior", *Res Mechanica*, **18**, 251 (1986).

31. Thrasher, M.A., Shahin, A.R., Meckl, P.H., and Jones, J.D., "Thermal Cycling of Shape Memory Alloy Wires using Semiconductor Heat Pump Modules", *Proceedings of the 1st European Conference on Smart Structures and Materials*, Glasgow, England (1992).

32. Wada, B.K., Fanson, J.L. and Crawley, E.F., "Adaptive Structures", *Journal of Intell. Mater. Sys. and Struct.*, **1**, 157 (1990).

33. Wayman, C.M., "Phase Transformations, Nondiffusive",in *Physical Metallurgy*, Eds: Cahn, R.W. and Haasen, P. ", North-Holland Physics Publishing, NY, 1301 (1983).

APPENDIX

A.Determination of material parameters for the thermodynamic theory

The method of determination of the parameters $\rho_{sma}\Delta s$, $\rho_{sma}\Delta u(\xi)$, first used in Eq.(2.12), and Y in Eq.(2.18) from experiments are given.

Determination of $\rho_{sma}\Delta s$

The parameter $\rho_{sma}\Delta s$ can be found by doing an uniaxial tensile test at the onset of transformation for which $\dot{\xi} = 0$. From Eq.(2.17), we have

$$\frac{d\sigma}{dT} = -\frac{\rho_{sma}\Delta s}{(E_M^{-1} - E_A^{-1})\sigma + (\alpha_M^{th} - \alpha_A^{th})\Delta T + H} , \tag{A.1}$$

where the total uniaxial inelastic strain, H, can be determined from an uniaxial tensile test of the polycrystal. Assuming that $(E_M^{-1} - E_A^{-1})\sigma + (\alpha_M^{th} - \alpha_A^{th})\Delta T << H$, Eq.(A.1) becomes

$$\frac{d\sigma}{dT} = -\frac{\rho_{sma}\Delta s}{H} .$$

In the $\sigma - T$ plane, a locii of points, usually a straight line(McCormick and Liu,1994), can be identified which represents the stresses at different temperatures for which the material starts to transform. Denoting the slope $\frac{d\sigma}{dT} = \mathrm{D}$, we have

$$\rho_{sma}\Delta s = -HD . \tag{A.2}$$

While several mechanical tests are needed to establish the line and hence determine D, it is easier to establish its value from a purely thermal transformation; this is addressed shortly.

Determination of $\rho_{sma}\Delta u(\xi)$

$\rho_{sma}\Delta u(\xi)$ can be determined from a purely thermal transformation, with $\sigma = 0$ and $\dot{\sigma} = 0$. The Eq.(2.11) reduces to

$$\dot{\xi} = \frac{\rho_{sma}\Delta s}{\rho_{sma}\frac{\partial \Delta u(\xi)}{\partial \xi}}\dot{T} . \tag{A.3}$$

where during a purely thermal transformation, we define

$$\frac{\rho_{sma}\Delta s}{\rho_{sma}\frac{\partial \Delta u(\xi)}{\partial \xi}} = a_p p(T) \ . \tag{A.4}$$

The parameter a_p is

$$a_p = -(1-\xi_0) \quad \dot{\xi} > 0 \qquad \text{and} \qquad a_p = -\xi_0 \quad \dot{\xi} < 0 \ , \tag{A.5}$$

where $\xi = \xi_0$ at the onset of transformation. The function $p(T)$ is taken to be a normal distibution, given as(Bhattacharyya and Lagoudas,1995)

$$p(T) = \frac{1}{b_p} exp\left[-\frac{1}{2}\left(\frac{T-0.5(T_l+T_h)}{s_p}\right)^2\right] \qquad T_l \leq T \leq T_h \ , \tag{A.6}$$

where s_p is the standard deviation and

$$b_p = \int_{T_l}^{T_h} exp\left[-\frac{1}{2}\left(\frac{T-0.5(T_l+T_h)}{s_p}\right)^2\right] dT \ .$$

The function defined by Eq.(A.6) satisfies the following condition

$$\int_{T_l}^{T_h} p(T)dT = 1 \ .$$

The temperatures T_l and T_h are

$$T_l = M_f^0 \qquad \text{and} \qquad T_h = M_s^0 \quad \text{for} \quad \dot{\xi} > 0,$$

and

$$T_l = A_s^0 \qquad \text{and} \qquad T_h = A_f^0 \quad \text{for} \quad \dot{\xi} < 0 \ ,$$

where M_s^0 and M_f^0 are the stress-free martensitic start and finish temperatures, A_s^0 and A_f^0 are the austenitic start and finish temperatures. Using the relation $\dot{\xi} = a_p p(T)\dot{T}$(from Eqs.(A.3)-(A.4)), conceptually it is possible to define $T = f(\xi)$. Since for a purely thermal transformation, using Eq.(A.2), Eq.(2.17) reduces to $\Pi = \rho_{sma}\Delta s T - \rho_{sma}\Delta u(\xi) = -HDT - \rho_{sma}\Delta u(\xi)$, we can write

$$\rho_{sma}\Delta u(\xi) = -HDf(\xi) \mp Y \ , \quad \text{for} \quad \dot{\xi} \gtrless 0 \ ,$$

where Eq.(2.18) has been used. D and Y are determined next. An analytical expression for $f(\xi)$ is not possible to derive when $p(T)$ is a normal distribution; a numerical procedure is then required to determine $f(\xi)$ at any arbitrary ξ.

Determination of D and Y

For a purely thermal transformation($\sigma = 0$ and $\dot{\sigma} = 0$), Eqs.(2.15), (2.17a), (A.3) and (A.4), give

$$-\nabla.q + r - C\dot{T} = a_p(\rho_{sma}\Delta sT - \Pi)p(T)\dot{T} \ . \tag{A.7}$$

The total latent heat evolved is defined as

$$H_l = \int(-\nabla.q + r - C\dot{T})dt \ , \tag{A.8}$$

where

$$H_l = \overset{+}{-} a_p H_a \qquad \text{for} \qquad \dot{\xi} \gtrless 0 \ , \ H_a > 0 \ . \tag{A.9}$$

The parameter H_a is the magnitude of the latent heat measured in a Differential Scanning Calorimetric(DSC) experiment during a $A \rightarrow M$ transformation of a SMA polycrystal in an initially austenitic state(or vice-versa); we have assumed for simplicity that the latent heat involved is identical for both transformations. Eqs.(A.7)-(A.9) yield

$$D = -2\frac{H_a}{H}\left[\int_{M_s^0}^{M_f^0} Tp(T)dT - \int_{A_s^0}^{A_f^0} Tp(T)dT\right]^{-1} \text{ and } Y = \frac{1}{2}HD\left[\int_{M_s^0}^{M_f^0} Tp(T)dT + \int_{A_s^0}^{A_f^0} Tp(T)dT\right]. \tag{A.10}$$

B. The parameters $G(t)$, $\mu(\xi,\sigma,T)$, $\nu_2(t)$, ν_1 and $F(t)$ and the correcponding nondimensional parameters

The parameters needed in Eq.(5.4) are

$$G(t) = \sum_{m=1}^{\infty} \overset{\cdot\cdot}{EXP}\left\{-\frac{\kappa_p}{C_p}\left[\left(\frac{m\pi}{d_p}\right)^2 + \frac{2h}{\kappa_p}\left(\frac{1}{b}+\frac{1}{w}\right)\right]t\right\} \ ,$$

$$\mu(\xi,\sigma,T) = \frac{dd_p}{4\kappa_p}C(\xi) \qquad \dot{\xi} = 0 \ ,$$

$$\mu(\xi,\sigma,T) = \frac{dd_p}{4\kappa_p}\left\{C(\xi) + \gamma(\sigma,T)\left[\sqrt{\rho_{sma}\frac{\partial\Delta u(\xi)}{\partial\xi}}\right]^{-1}\psi(\xi) + \right.$$

$$\left.\left[\alpha^{th}(\xi)T(t) + \gamma(\sigma,T)\left[\sqrt{\rho_{sma}\frac{\partial\Delta u(\xi)}{\partial\xi}}\right]^{-1}\beta(\xi,\sigma,T)\right]s(\xi,\sigma,T)\right\} \qquad \dot{\xi} \neq 0 \ ,$$

$$\nu_2(t) = \frac{d_p}{2\kappa_p}\alpha_p J(t) + \frac{1}{2} + \frac{hdd_p}{2\kappa_p}\left(\frac{1}{b}+\frac{1}{w}\right) \ , \ \nu_1 = 2\frac{h}{C_p}\left(\frac{1}{b}+\frac{1}{w}\right) \ ,$$

$$F(t) = \frac{2hT_0}{C_p}\left(\frac{1}{b}+\frac{1}{w}\right)\int_0^t G(t-\tau)d\tau + \frac{2\rho_p}{C_p}\int_0^t H(t-\tau)J(\tau)^2 d\tau + \frac{T_0}{2} + \frac{hdd_pT_0}{2\kappa_p}\left(\frac{1}{b}+\frac{1}{w}\right) + \frac{\rho dd_p}{4\kappa_p}J(t)^2 ,$$

$$H(t) = \sum_{m=1}^{\infty} EXP\left\{-\frac{\kappa_p}{C_p}\left[\left(\frac{(2m-1)\pi}{d_p}\right)^2 + \frac{2h}{\kappa_p}\left(\frac{1}{b}+\frac{1}{w}\right)\right]t\right\} . \qquad \text{(A.11)}$$

whereas those in Eq.(5.23) are

$$\bar{G}(\bar{t}) = G(t) \ , \ \bar{\mu}(\xi,\bar{\sigma},\bar{T}) = \left(\frac{C_p d_p^2}{\kappa_p}\right)^{-1}\mu(\xi,\sigma,T) \ , \ \bar{\nu}_2(\bar{t}) = \nu_2(t) \ ,$$

$$\bar{\nu}_1 = \frac{C_p d_p^2}{\kappa_p}\nu_1 \ , \ \bar{F}(\bar{t}) = \frac{1}{T_0}F(t) \ , \ \bar{H}(\bar{t}) = H(t) \ . \qquad \text{(A.12)}$$

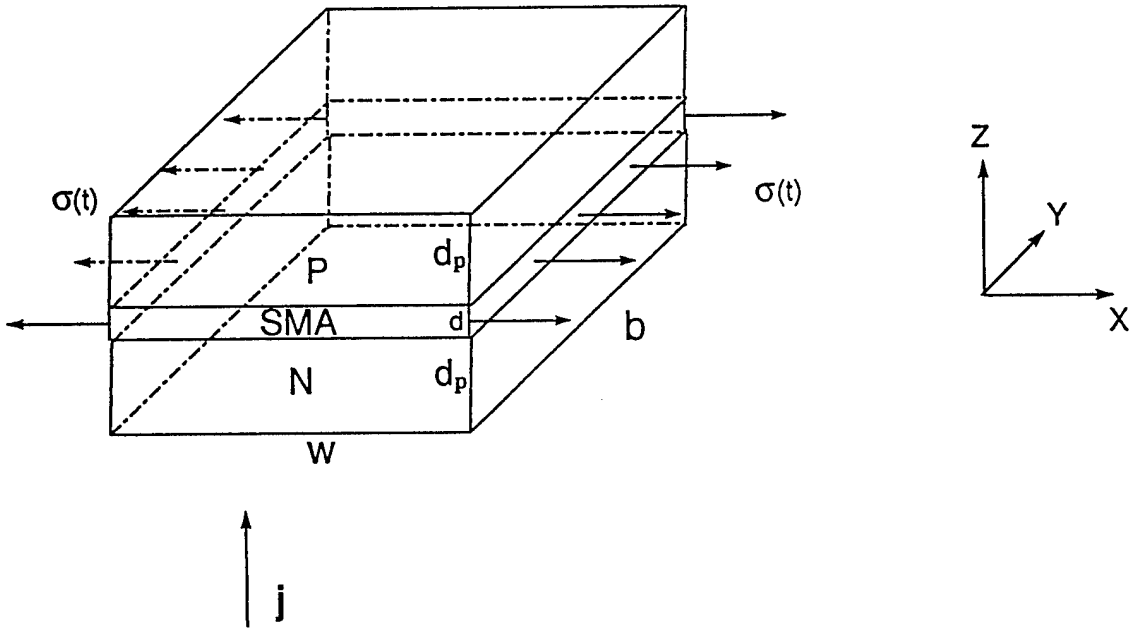

Figure 1. Schematic diagram of a thin layer extensional SMA actuator with P and N semiconductor thermoelectric elements.

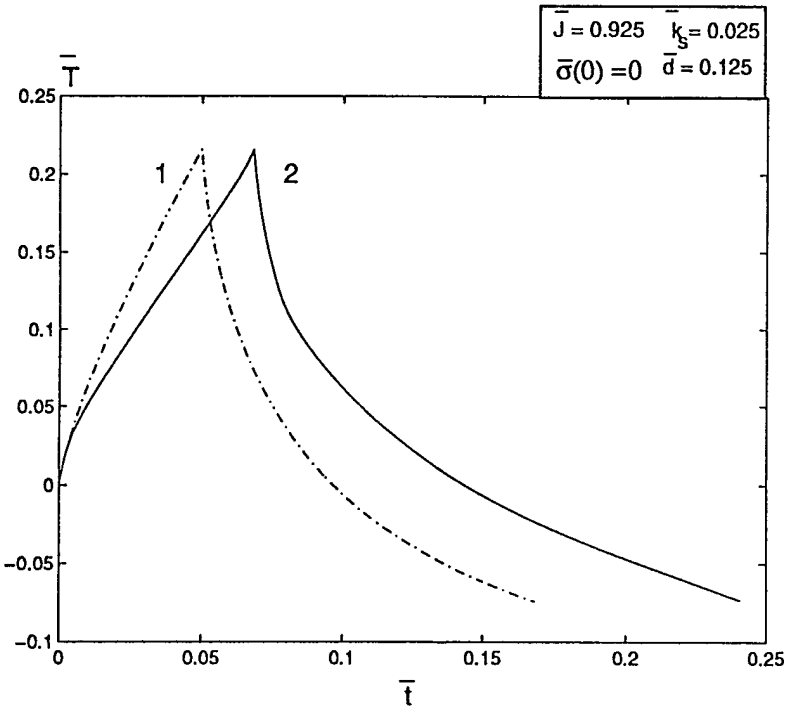

(a)

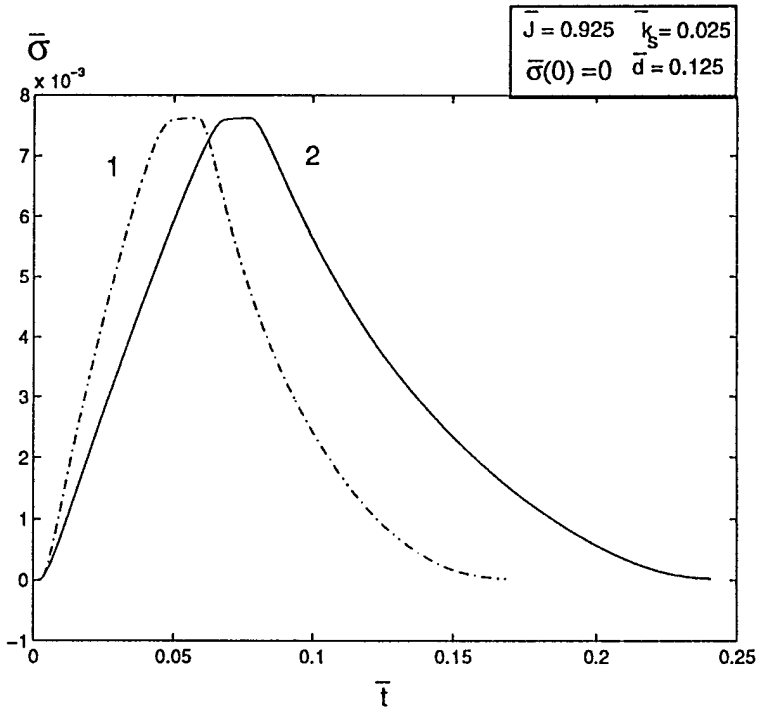

(b)

Figure 2. The influence of the coupling terms on the nondimensional temperature and stress profiles.

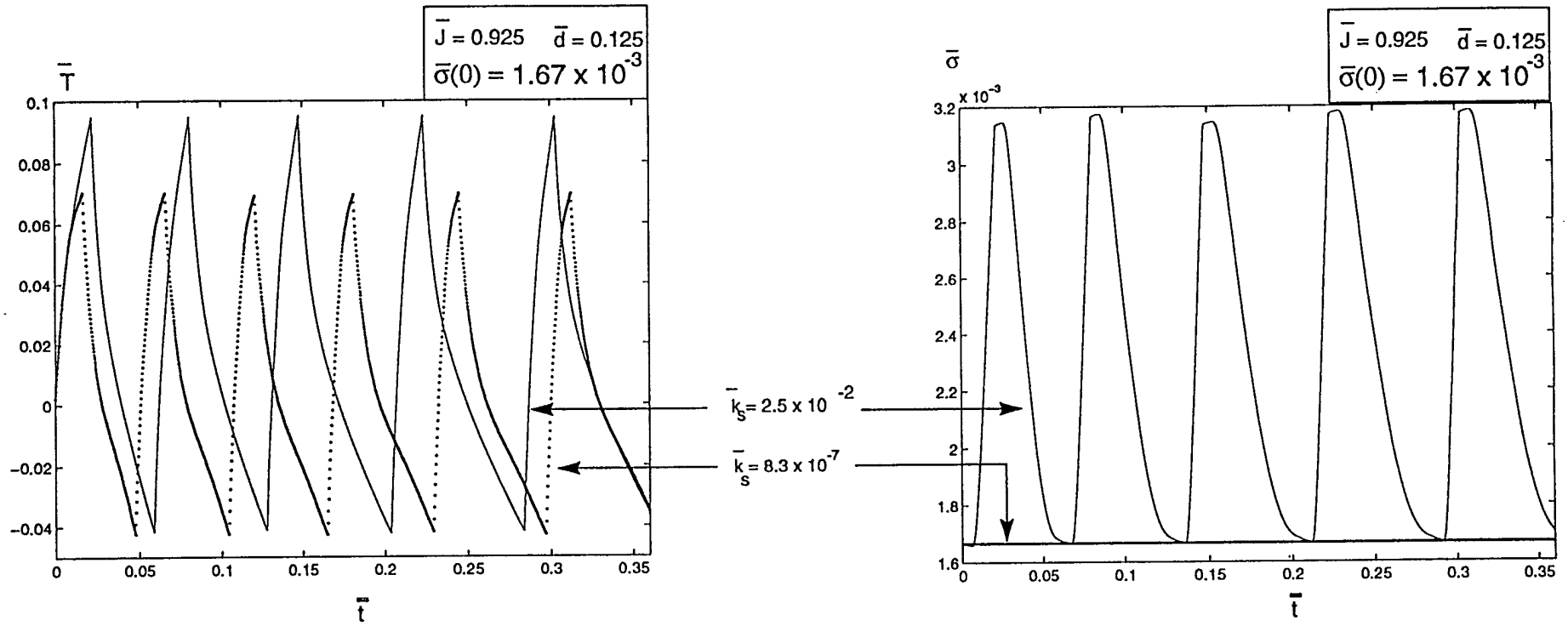

(a) (b)

Figure 3 (a) Nondimensional temperature profiles corresponding to nondimensional spring stiffnesses $\bar{k}_s = 8.3 \times 10^{-7}$ and 2.5×10^{-2} and (b) the evolution of the nondimensional stresses.

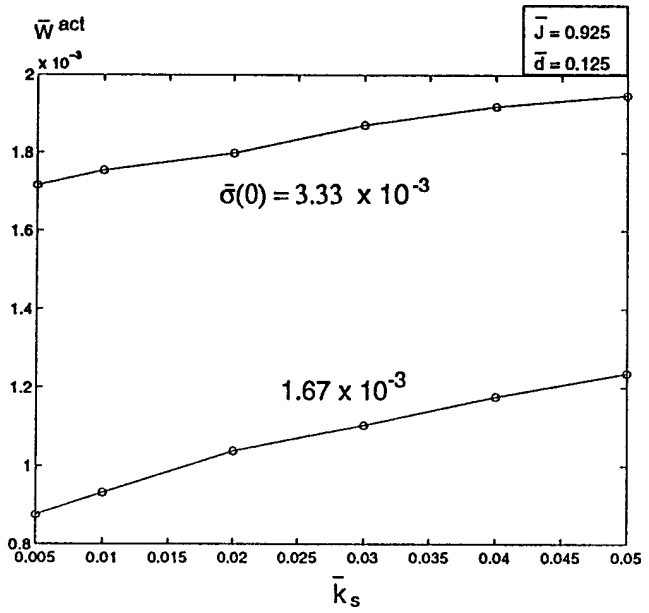

(a)

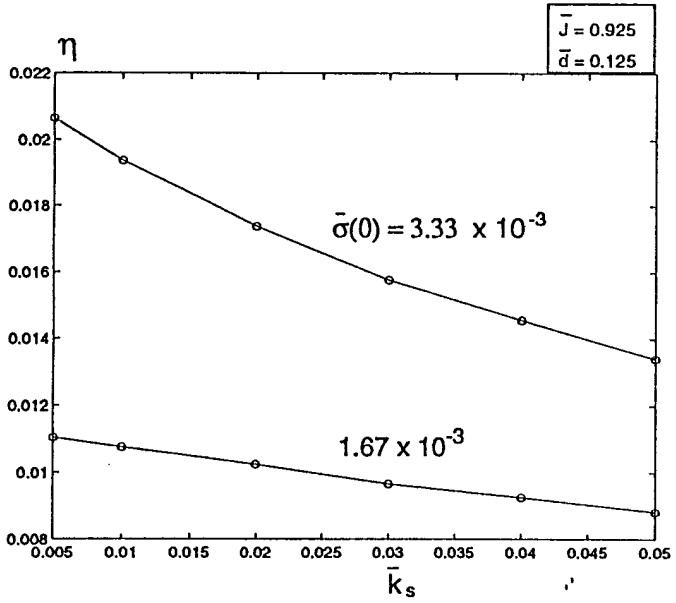

(b)

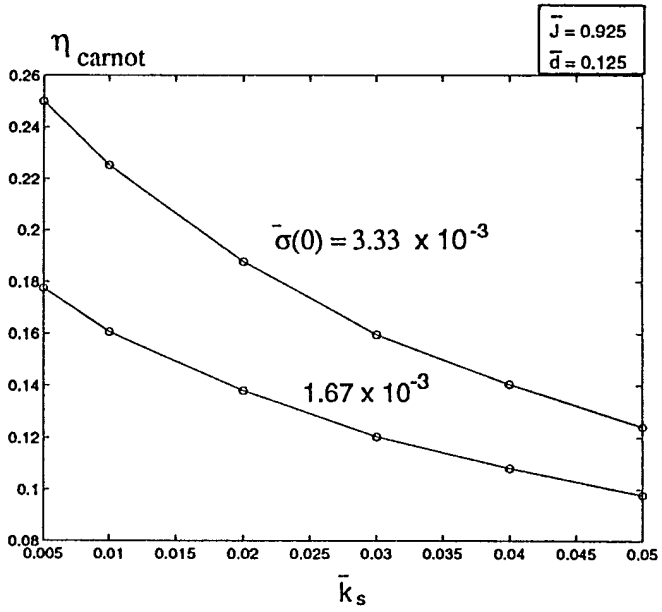

(c)

Figure 4. (a) Nondimensional mechanical work output, (b) energy efficiencies, and (c) the corresponding carnot efficiencies.

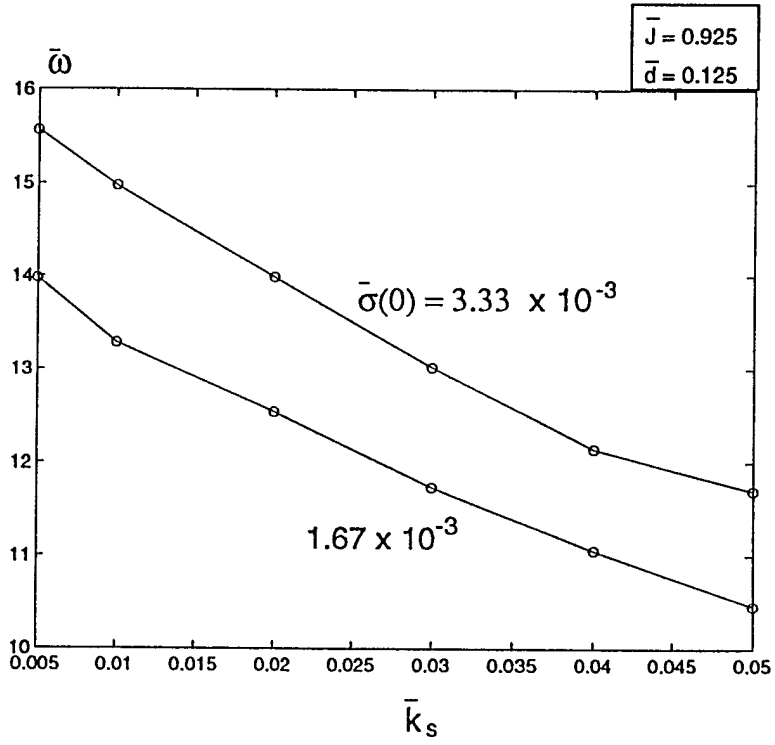

Figure 5. Nondimensional frequency of actuation at two stress levels for a range of spring stiffnesses.

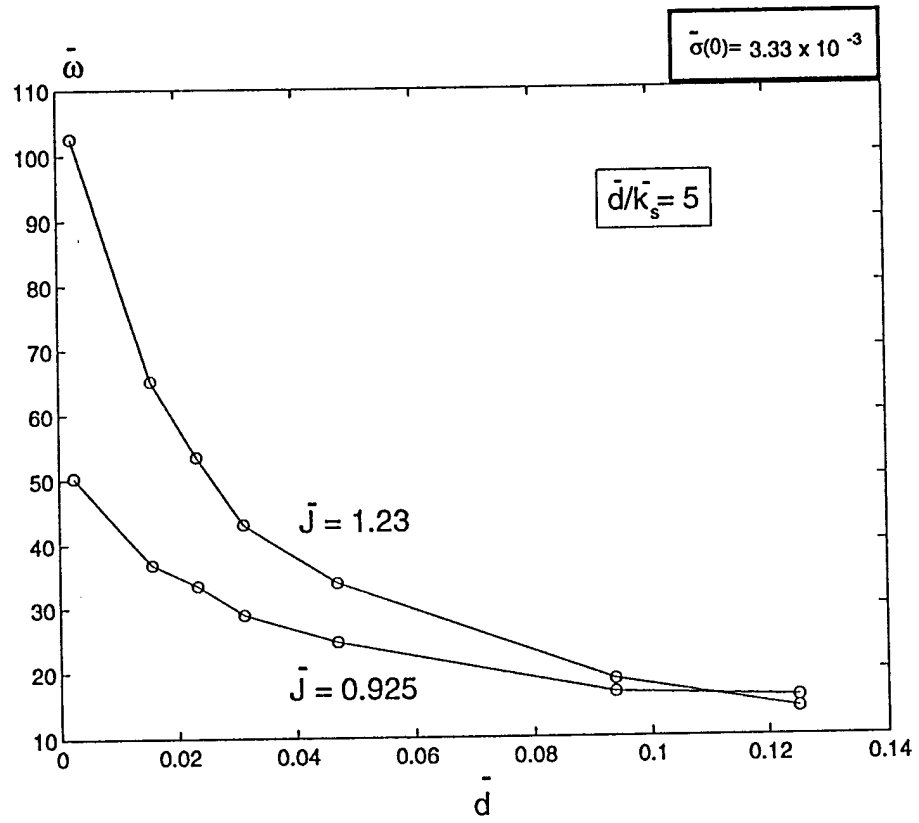

Figure 6. Nondimensional frequency of actuation at two current levels for a range of nondimensional SMA layer thicknesses.

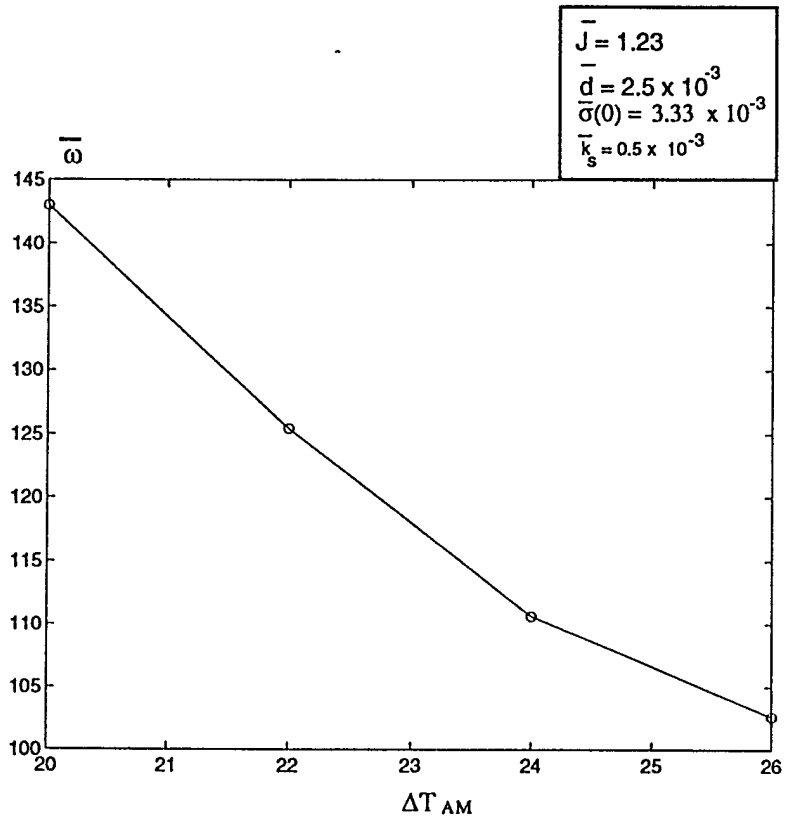

Figure 7. The nondimensional frequency of actuation as a function of the hysteresis in the transformation temperatures.

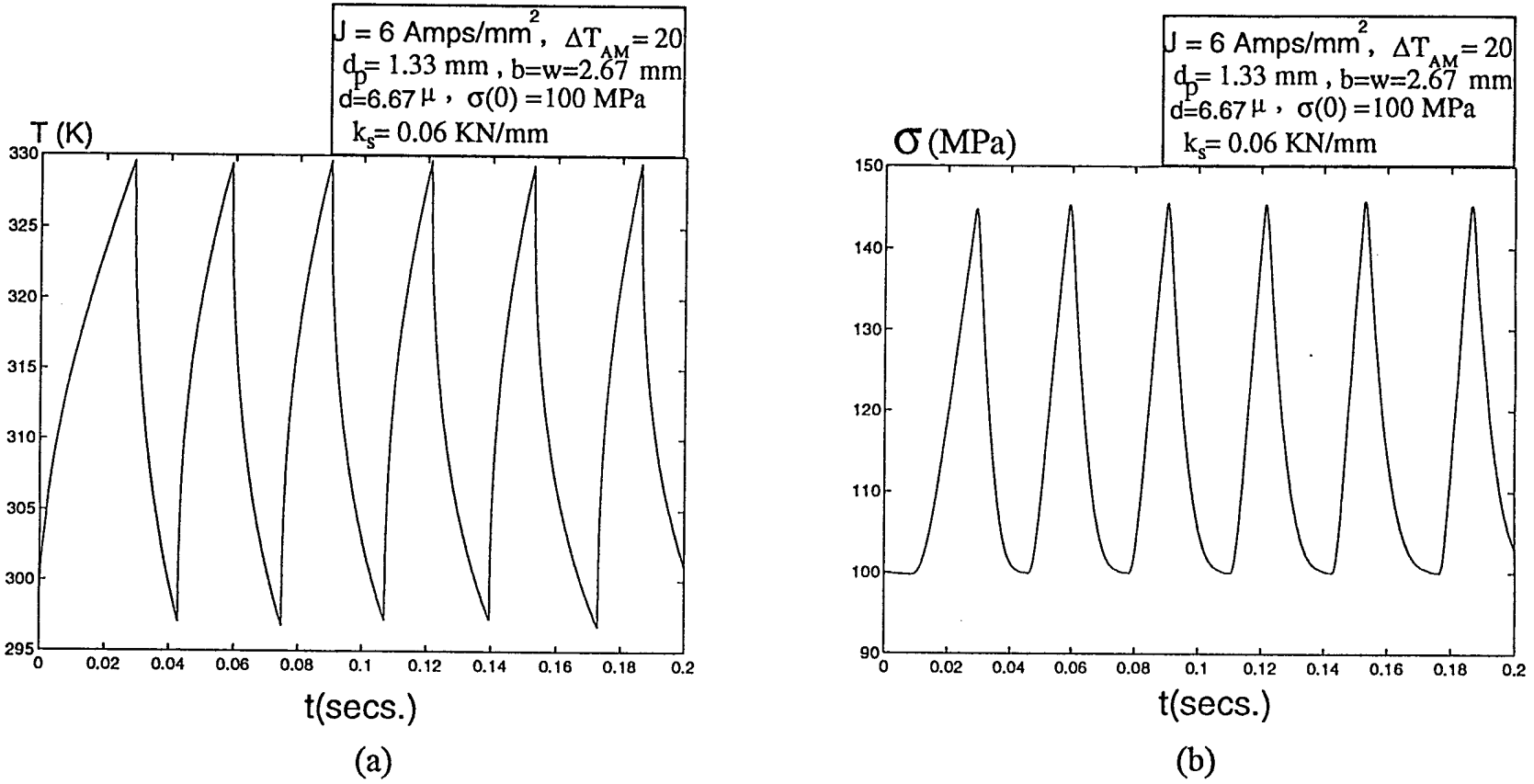

Figure 8. (a) The dimensional temperature vs. time and (b) dimensional stress vs. time.